EUROPEAN ORGANIZATION FOR NUCLEAR RESEARCH

Observation of a multiplicity dependence in the p_T-differential charm baryon-to-meson ratios in proton–proton collisions at $\sqrt{s} = 13$ TeV

ALICE Collaboration*

Abstract

The production of prompt D^0, D_s^+, and Λ_c^+ hadrons, and their ratios, D_s^+/D^0 and Λ_c^+/D^0, are measured in proton–proton collisions at $\sqrt{s} = 13$ TeV at midrapidity ($|y| < 0.5$) with the ALICE detector at the LHC. The measurements are performed as a function of the charm-hadron transverse momentum (p_T) in intervals of charged-particle multiplicity, measured with two multiplicity estimators covering different pseudorapidity regions. While the strange to non-strange D_s^+/D^0 ratio indicates no significant multiplicity dependence, the baryon-to-meson p_T-differential Λ_c^+/D^0 ratio shows a multiplicity-dependent enhancement, with a significance of 5.3σ for $1 < p_T < 12$ GeV/c, comparing the highest multiplicity interval with respect to the lowest one. The measurements are compared with a theoretical model that explains the multiplicity dependence by a canonical treatment of quantum charges in the statistical hadronisation approach, and with predictions from event generators that implement colour reconnection mechanisms beyond the leading colour approximation to model the hadronisation process. The Λ_c^+/D^0 ratios as a function of p_T present a similar shape and magnitude as the Λ/K_S^0 ratios in comparable multiplicity intervals, suggesting a potential common mechanism for light- and charm-hadron formation, with analogous multiplicity dependence. The p_T-integrated ratios, extrapolated down to $p_T = 0$, do not show a significant dependence on multiplicity within the uncertainties.

*See Appendix A for the list of collaboration members

1 Introduction

Heavy-flavour hadrons are produced in high-energy particle collisions through the hadronisation of the corresponding heavy-flavour quarks, which in turn typically originate from early hard scattering processes. The most common theoretical approach to describe this production is based on the quantum chromodynamics (QCD) factorisation theorem [1]. In this framework, the production of hadrons containing charm or beauty quarks is calculated as a convolution of three independent terms: the parton distribution functions of the incoming protons, the cross sections of the partonic scatterings producing the heavy quarks, and the fragmentation functions that parametrise the non-perturbative evolution of a heavy quark into a given species of heavy-flavour hadron. Calculations based on the factorisation approach rely on the assumption that fragmentation functions, which are typically measured in e^+e^- or e^-p collisions [2], are universal across all collision systems and energies. Systematic measurements of the relative production of heavy-flavour hadrons performed in different collision systems provide an excellent experimental benchmark to test this assumption.

Perturbative calculations at next-to-leading order, with next-to-leading-log resummation [3–6], can successfully describe the production cross section of strange and non-strange charm mesons and their ratios, as a function of transverse momentum (p_T) and rapidity in proton–proton (pp) collisions, over a wide range of centre-of-mass energies [7–11]. In contrast, these calculations, which are based on collinear factorisation and fragmentation functions tuned on e^+e^- and e^-p collision measurements, provide a poor description of heavy-flavour baryon production in hadronic collisions. Measurements of the Λ_c^+ production cross section in pp collisions at centre-of-mass energies of $\sqrt{s} = 7$, 5.02, and 13 TeV [12–15] have shown a larger p_T-differential cross section compared to QCD calculations [3, 4, 16] as well as higher values for the Λ_c^+/D^0 ratio with respect to e^+e^- collision data from LEP [17]. Similarly, a Λ_c^+/D^0 ratio larger than expectations from e^+e^- collisions was measured in p–Pb collisions at the LHC, both at midrapidity by ALICE [12, 13] and at forward rapidity by the LHCb experiment [18].

In particular, the measurements in pp collisions at $\sqrt{s} = 5.02$ and 13 TeV provided the statistical precision to discriminate among different theoretical approaches. The measurements show, with good accuracy, a decrease of the Λ_c^+/D^0 ratio from about 0.6 in the interval $1 < p_T < 2$ GeV/c to about 0.3 for $8 < p_T < 12$ GeV/c. Calculations based on PYTHIA 8 [19] with Monash tune [20] and HERWIG 7 [21], in which the charm fragmentation is tuned to e^+e^- and e^-p measurements, cannot describe the experimental results since they predict a p_T-independent Λ_c^+/D^0 ratio of about 0.1. A much better agreement is achieved by PYTHIA 8 calculations that include colour reconnection mechanisms beyond the leading-colour approximation [22] (CR-BLC in the following). These calculations introduce new colour-reconnection topologies enhancing the contribution of "junctions" that fragment into baryons, thus providing an augmented baryon production. Calculations based on the statistical hadronisation model [23] or calculations that include mechanisms of charm-hadron formation through coalescence of constituent quarks in the presence of a colour-deconfined state of matter [24], also provide a satisfactory description of the Λ_c^+/D^0 ratio in pp collisions. This suggests the presence of modified or additional hadronisation mechanisms in small hadronic collision systems with respect to fragmentation in vacuum. Similar conclusions are drawn from recent measurements of higher-mass charm-baryon states, $\Xi_c^{0,+}$ and $\Sigma_c^{0,++}$, in pp collisions at $\sqrt{s} = 5.02$, 7, and 13 TeV [15, 25–27]. The fragmentation fractions, i.e. the probabilities for a charm quark to hadronise into a specific charm hadron, computed for the first time from hadronic collision measurements at the LHC including the charm baryon states, are found to be different than those measured in e^+e^- and e^-p collisions. This observation confirms that the hadronisation of charm quarks into charm hadrons is not a universal process among different collision systems [28].

The measurements of the Λ_c^+/D^0 and D_s^+/D^0 ratios also play an important role in the study of heavy-ion collisions, where a hot and dense quark–gluon plasma, characterised by the presence of free colour charges, is formed [29]. In heavy-ion collisions, measurements of baryon-to-meson ratios and of strange to non-strange hadron production ratios [14, 30–37] are sensitive to the mechanisms of hadronisation

2

from the quark–gluon plasma [38]. A first measurement of the Λ_c^+/D^0 ratio in Pb–Pb collisions, in the 80% most central collisions, was performed at $\sqrt{s_{NN}} = 5.02$ TeV [32] by ALICE. The measurement is consistent with the hypothesis of an enhancement of the Λ_c^+/D^0 ratio with respect to pp collisions in the intermediate p_T region $6 < p_T < 12$ GeV/c, although the limited statistical precision does not yet allow for a firm conclusion to be drawn. The Λ_c^+/D^0 ratio in heavy-ion collisions was also measured by CMS, in Pb–Pb collisions at $\sqrt{s_{NN}} = 5.02$ TeV for $10 < p_T < 20$ GeV/c [14], and by STAR, in Au–Au collisions at $\sqrt{s_{NN}} = 200$ GeV for $2.5 < p_T < 8$ GeV/c [33]. While the STAR result is significantly higher than PYTHIA 8 calculations with different tunes [20, 22], the CMS ratio at higher p_T is consistent with the pp result. A hint of enhancement of the D_s^+/D^0 ratio in central Pb–Pb collisions with respect to pp collisions was also observed at $\sqrt{s_{NN}} = 5.02$ TeV in the intermediate p_T region $4 < p_T < 8$ GeV/c, as expected in the presence of a sizeable contribution of coalescence processes and increased strangeness production in the medium [35, 36]. A similar conclusion is drawn by STAR from the measured D_s^+/D^0 ratio in the 10% most central Au–Au collisions at $\sqrt{s_{NN}} = 200$ GeV relative to PYTHIA simulation of pp collisions [37]. A measurement performed in high-multiplicity pp collisions could shed light on the possible presence of similar effects also in smaller collision systems with large particle densities.

In this Letter, we present the first measurement of the production yields of prompt D^0, D_s^+ and Λ_c^+ (i.e. produced in the hadronization of charm quarks or from the decay of excited open charm and charmonium states) as well as corresponding ratios, D_s^+/D^0 and Λ_c^+/D^0, in pp collisions at $\sqrt{s} = 13$ TeV, as a function of the charged-particle pseudorapidity density $\langle dN_{ch}/d\eta \rangle$. The aim of this study is to characterise the evolution of the aforementioned ratios from very low to moderate charged-particle density and provide new experimental constraints on the nature of these modifications in small systems. The study was performed considering events selected according to the charged-particle density at mid- and forward rapidities, in order to investigate the effects of possible biases originating from the determination of the multiplicity in the same pseudorapidity region in which charm hadrons are reconstructed. Comparisons with theoretical calculations and Monte Carlo simulations are also provided. In addition, the Λ_c^+/D^0 results are compared to Λ/K_S^0 measurements in similar multiplicity intervals [39]. The p_T-integrated Λ_c^+/D^0 yield ratios, extrapolated down to $p_T = 0$, are also presented.

2 Experimental apparatus and data samples

The ALICE experiment and its performance are presented in detail in Refs. [40, 41]. The main detectors considered for the measurements discussed in this paper are the Inner Tracking System (ITS) for tracking, vertex reconstruction, event multiplicity estimation, and trigger purposes; the Time Projection Chamber (TPC) for tracking and particle identification; the Time-Of-Flight (TOF) for particle identification; and the V0 detector for event multiplicity estimation as well as for trigger purposes.

The event multiplicity selection was based on two estimators. At midrapidity ($|\eta| < 1$) the multiplicity was estimated via the number of tracklets (N_{trkl}) defined as track segments built by associating pairs of hits in the two Silicon Pixel Detector (SPD) layers, which are the two innermost layers of the ITS. The acceptance of the SPD in pseudorapidity changes with the longitudinal position of the vertex z_{vtx} and, in addition, the acceptance-times-efficiency changes with time due to variations of the inactive channels. Therefore, a data-driven correction procedure was applied on an event-by-event basis to N_{trkl}, depending on the z_{vtx} position and the data taking period, as further described in Ref. [42]. The event multiplicity in the forward rapidity region was estimated from the percentile distribution p_{V0M} of the V0M amplitude, which is the sum of signal amplitudes in the V0A and V0C scintillators. They are the two detecting components of the V0 detector on opposite sides of the interaction point along the beam axis, covering the pseudorapidity regions of $2.8 < \eta < 5.1$ and $-3.7 < \eta < -1.7$, respectively. The p_{V0M} values towards 0 correspond to the highest multiplicity events, while the lowest are assigned a value towards 100%.

The data from pp collisions at $\sqrt{s} = 13$ TeV used for this analysis were collected in the years 2016, 2017, and 2018. Three trigger setups were employed. The minimum-bias (MB) trigger required signals in both V0A and V0C in coincidence with the proton bunch arrival time. To enrich the data sample in the highest multiplicity regions, high-multiplicity triggers based on a minimum selection of the number of hits in the SPD (HMSPD) or of V0 amplitudes (HMV0) were used, which were fully efficient for $N_{\mathrm{trkl}} > 65$ and $p_{\mathrm{V0M}} < 0.1\%$, respectively.

Offline selection criteria were applied in order to remove background events from beam–gas collisions and other machine-induced background as described in Ref. [43]. To reduce the contamination from events with superposition of more than one collision within the colliding bunches (pile-up), events with multiple reconstructed primary vertices were rejected. The impact of potentially remaining pile-up events is on the percent level and does not influence the final results of the present analysis. Only events with a vertex position of $|z_{\mathrm{vtx}}| < 10$ cm around the nominal interaction point were considered to ensure a uniform acceptance. In addition, events were required to have at least one reconstructed tracklet within the pseudorapidity region $|\eta| < 1$ (INEL > 0 event class). This class of events minimises diffractive corrections and has a high trigger efficiency. It corresponds to about 75% of the total inelastic cross section [43, 44]. After the aforementioned selections, the integrated luminosity of the data sample is about 32 nb^{-1} for the MB triggered events. Only the data periods granting an uniform efficiency of the HMV0 and HMSPD triggers, inside the range covered by the multiplicity intervals considered in the analysis, were used, resulting in an integrated luminosity of about 7.7 pb^{-1} with HMV0 and 0.8 pb^{-1} for the HMSPD trigger sample.

The events were assigned to multiplicity intervals based on the corresponding observables N_{trkl} and p_{V0M}, as presented in Table 1. The last N_{trkl} and p_{V0M} intervals contain data collected with the HMSPD and HMV0 triggers, respectively. To account for a possible trigger inefficiency for HMSPD triggered events in the range $60 < N_{\mathrm{trkl}} < 65$, a correction was applied with a data-driven reweighting procedure, as described in Ref. [42].

The mean multiplicity density ($\langle \mathrm{d}N_{\mathrm{ch}}/\mathrm{d}\eta \rangle_{|\eta|<0.5}$) of charged primary particles, whose definition is given in Ref. [45], was obtained by converting the measured event multiplicities as described in Ref. [43]. For the p_{V0M} percentiles the values reported in Ref. [43] were used. The conversion of the specific N_{trkl} intervals used in this analysis was performed by means of a PYTHIA [19] Monte Carlo (MC) simulation, with particle transport based on the GEANT3 package [46], and by selecting the charged primary particles measured at midrapidity in the events corresponding to the given N_{trkl} intervals. Throughout the analysis reported in this paper, PYTHIA 8.243 with Monash tune [20] was used; the version will not be reported later for the sake of simplicity.

A summary of the above information is given in Table 1 together with the trigger correction $\varepsilon^{\mathrm{INEL}}$ to account for those events which fulfil the INEL > 0 requirement but were not selected by the trigger, as specified in Ref. [43].

3 Data Analysis

The D^0, D_s^+, and Λ_c^+ hadrons and their charge conjugates were reconstructed via the hadronic decay channels $D^0 \to K^-\pi^+$ (branching ratio BR = $(3.950 \pm 0.031)\%$), $D_s^+ \to \phi\pi^+ \to K^+K^-\pi^+$ (BR = $(2.24 \pm 0.08)\%$), $\Lambda_c^+ \to pK^-\pi^+$ (BR = $(6.28 \pm 0.32)\%$), and $\Lambda_c^+ \to pK_S^0 \to p\pi^+\pi^-$ (BR = $(1.10 \pm 0.06)\%$) [47]. The analysis was performed for the different multiplicity intervals, as defined in Table 1. Transverse-momentum intervals between 1 and 24 GeV/c were chosen to guarantee a large statistical significance in all multiplicity event classes. In order to minimise systematic effects, which could have a different impact in the different multiplicity intervals considered in the analysis, the same event and candidate selection criteria were used in all the multiplicity classes. The charm-hadron decay tracks were excluded from the N_{trkl} estimation at midrapidity, in order to reduce the effects of auto-correlation that could arise

Table 1: Summary of the multiplicity event classes at midrapidity (N_{trkl}) and forward rapidity (p_{V0M} [%]), the latter corresponding to the visible V0M cross section. The average charged-particle densities $\langle \mathrm{d}N_{\mathrm{ch}}/\mathrm{d}\eta \rangle_{|\eta|<0.5}$ at midrapidity are shown, together with the value corresponding to the INEL > 0 event class. The trigger efficiency $\varepsilon^{\mathrm{INEL}}$ is also reported for each multiplicity interval, as estimated in Ref. [43].

Mult. estimator	Mult. interval	$\langle \mathrm{d}N_{\mathrm{ch}}/\mathrm{d}\eta \rangle_{|\eta|<0.5}$	$\varepsilon^{\mathrm{INEL}}$
N_{trkl}	$[1,9]$	3.10 ± 0.02	0.862 ± 0.015
	$[10,29]$	10.54 ± 0.01	0.997 ± 0.002
	$[30,59]$	22.56 ± 0.07	1 (negl. unc.)
	$[60,99]$	37.83 ± 0.06	1 (negl. unc.)
p_{V0M} [%]	$[30,100]$	4.41 ± 0.05	0.897 ± 0.013
	$[0.1,30]$	13.81 ± 0.14	0.997 ± 0.001
	$[0,0.1]$	31.53 ± 0.38	1 (negl. unc.)
INEL > 0		6.93 ± 0.09	0.920 ± 0.003

from the measurement of the charged-particle distribution in the same pseudorapidity region as the charm hadrons. A possible remaining bias could be induced by the charged particles produced in the fragmentation of the charm quarks or by decays of excited charm states that are not subtracted from the N_{trkl} count.

$\mathrm{D}^0 \rightarrow \mathrm{K}^- \pi^+$, $\mathrm{D}_{\mathrm{s}}^+ \rightarrow \phi \pi^+ \rightarrow \mathrm{K}^+ \mathrm{K}^- \pi^+$, and $\Lambda_{\mathrm{c}}^+ \rightarrow \mathrm{p} \mathrm{K}^- \pi^+$ candidates were defined by combining pairs or triplets of tracks with the proper charge signs, while the reconstruction of the $\Lambda_{\mathrm{c}}^+ \rightarrow \mathrm{p} \mathrm{K}_{\mathrm{S}}^0$ candidates relied on reconstructing the V-shaped decay of the $\mathrm{K}_{\mathrm{S}}^0$ meson into two pions, which was then combined with a proton-candidate track. Track-quality selections were applied to the candidate daughters as explained in Ref. [13]. As a consequence of these track-selection criteria, the detector acceptance for D mesons and Λ_{c}^+ baryons varies as a function of rapidity, falling steeply to zero for $|y| > 0.5$ at low p_{T} and for $|y| > 0.8$ at $p_{\mathrm{T}} > 5$ GeV/c. For this reason, a fiducial acceptance selection was applied on the rapidity of the candidates, $|y| < y_{\mathrm{fid}}(p_{\mathrm{T}})$, where the factor $y_{\mathrm{fid}}(p_{\mathrm{T}})$ was defined as a second-order polynomial function, increasing from 0.5 to 0.8 in the transverse-momentum range $0 < p_{\mathrm{T}} < 5$ GeV/c, and as a constant term, $y_{\mathrm{fid}} = 0.8$, for $p_{\mathrm{T}} > 5$ GeV/c. The correction factors for the acceptance were computed accordingly. Further selections on the charm-hadron decay topology and on the particle identification (PID) of their decay products were exploited to reduce the combinatorial background. The same selection criteria described in Refs. [11, 13] were used for D^0 and $\Lambda_{\mathrm{c}}^+ \rightarrow \mathrm{p} \mathrm{K}^- \pi^+$, while for the $\mathrm{D}_{\mathrm{s}}^+$ and $\Lambda_{\mathrm{c}}^+ \rightarrow \mathrm{p} \mathrm{K}_{\mathrm{S}}^0$ analyses, a machine-learning approach with Boosted Decision Trees (BDTs), using the toolkit from XGBoost [48], was employed. Binary BDT classifiers were used and the training sample was assembled considering the background from the sidebands of the candidate invariant-mass distribution in data, and the prompt signal candidates from MC simulations based on the PYTHIA Monash event generator. Independent BDTs were trained for each p_{T} interval in the multiplicity-integrated sample. The most prominent variables that were used in the training for the Λ_{c}^+ analysis are related to the PID of the proton decay track, the reconstructed invariant mass and $c\tau$ of the $\mathrm{K}_{\mathrm{S}}^0$ candidate, the cosine of the pointing angle between the line of flight of the $\mathrm{K}_{\mathrm{S}}^0$ meson (the vector connecting the primary and secondary vertices) and its reconstructed momentum vector, and the distance between the $\mathrm{K}_{\mathrm{S}}^0$-meson decay vertex and the primary vertex. For the $\mathrm{D}_{\mathrm{s}}^+$ analysis, the variables provided to the BDTs are the same as reported in Ref. [49]. The selections on the BDT outputs were tuned to provide a large statistical significance for the signal.

The signal extraction was performed via binned maximum-likelihood fits to the invariant-mass distributions of candidates in each p_{T} and multiplicity interval. For all analyses, a Gaussian function was used to describe the signal peak. To model the background, an exponential function was used for the D^0 mesons and for $\mathrm{D}_{\mathrm{s}}^+$ mesons with a transverse momentum higher than 4 GeV/c, while a second-order polynomial

function was used for both Λ_c^+ decay channels as well for the lowest two p_T intervals of the D_s^+-meson analysis. Due to the limited number of candidates in some multiplicity classes and the large combinatorial background, it was not possible to extract the raw yield in the full p_T range for all the multiplicity intervals: the range $1 < p_T < 2$ GeV/c in the low and high multiplicity classes and $12 < p_T < 24$ GeV/c in the low multiplicity class are missing, respectively, for the D_s^+ and Λ_c^+ analyses. Examples of the invariant-mass distributions for D^0, D_s^+, $\Lambda_c^+ \to pK^-\pi^+$, and $\Lambda_c^+ \to pK_S^0$ candidates for the different p_T and multiplicity intervals are reported in Ref. [50].

The corrected per-event yields were computed for each p_T and multiplicity interval as

$$\frac{1}{N_{\text{mult}}^{\text{ev}}} \frac{\mathrm{d}N_{\text{mult}}^{\text{hadron}}}{\mathrm{d}p_T} = \frac{\varepsilon_{\text{mult}}^{\text{INEL}}}{N_{\text{mult}}^{\text{ev}}} \frac{1}{c_{\Delta y}(p_T) \times \Delta p_T} \frac{1}{\text{BR}} \frac{f_{\text{prompt}}(p_T) \times \frac{1}{2} \times N_{\text{mult}}^{\text{hadron,raw}}(p_T)\big|_{|y| < y_{\text{fid}}(p_T)}}{(\text{Acc} \times \varepsilon)_{\text{prompt,mult}}(p_T)}, \quad (1)$$

where $N_{\text{mult}}^{\text{hadron,raw}}$ is the raw yield (sum of particles and antiparticles) extracted in a given p_T and multiplicity interval. It is multiplied by the prompt fraction f_{prompt} in order to correct for the corresponding beauty-hadron decay contribution, and divided by the multiplicity-dependent prompt acceptance-times-efficiency, $(\text{Acc} \times \varepsilon)_{\text{prompt,mult}}$. It is further divided by a factor of two to obtain the charge-averaged yield, by the BR of the decay channel, the p_T-interval width (Δp_T), and the correction factor for the rapidity coverage $c_{\Delta y}$, computed as the ratio between the generated hadron yield in $\Delta y = 2y_{\text{fid}}$ and that in $|y| < 0.5$. The factor $N_{\text{mult}}^{\text{ev}}$ denotes the number of recorded events in each multiplicity class, which is then corrected for the fraction of INEL > 0 events that were not selected by the trigger, $\varepsilon_{\text{mult}}^{\text{INEL}}$, whose values are reported in Table 1.

The geometrical acceptance of the detector times the reconstruction efficiency ($\text{Acc} \times \varepsilon$), obtained separately for prompt and feed-down hadrons, was determined from pp collisions simulated with PYTHIA with Monash tune, with particle transport based on the GEANT3 package [46]. To account for the multiplicity dependence of the efficiency, which is driven by the primary-vertex resolution improving with increasing multiplicity, the generated events were weighted based on the number of tracklets in order to match the distribution observed in data. The generated Λ_c^+ p_T spectrum used to calculate the efficiencies was weighted to reproduce the shape obtained from the PYTHIA CR-BLC tune, which describes the measured spectra better than the Monash tune as observed in Ref. [13].

The estimated $(\text{Acc} \times \varepsilon)_{\text{prompt,mult}}$ varies between 0.5% and 60% depending on p_T and species, and increases with multiplicity [50]. The largest difference with respect to the efficiency computed in the INEL > 0 class is observed in $1 < p_T < 2$ GeV/c, where the discrepancy reaches 30% for D_s^+, while it steeply decreases to few percents with increasing p_T.

The f_{prompt} fraction was estimated as reported in Refs. [13, 49], using (i) the beauty-quark production cross section from FONLL calculations [5, 6], (ii) the $(\text{Acc} \times \varepsilon)$ for feed-down charm hadrons, (iii) beauty-quark fragmentation fractions determined from LHCb data [51] for $b \to \Lambda_b^0$ and from e^+e^- measurements [17] for $b \to B$, and (iv) modelling the decay kinematics with PYTHIA simulations. The f_{prompt} fraction was assumed to be independent of the event multiplicity and therefore computed for the minimum-bias event class. This assumption is justified by the expected weak dependence of the feed-down fraction with multiplicity [42], predicted also by PYTHIA, and the small variations of the efficiency for the feed-down of charm hadrons observed in the simulation for the different multiplicity intervals. The values of f_{prompt} range from 0.81 to 0.97 depending on p_T and particle species.

4 Systematic uncertainty evaluation

Sources of systematic uncertainty on the measured corrected yields were studied following procedures similar to those described in detail in Refs. [11, 13] for the minimum-bias Λ_c^+ and D-meson analyses. The multiplicity-independent sources, i.e. those related to the tracking efficiency, the PID selection and

the simulated charm-hadron p_T spectra, are discussed first, and then those related to the multiplicity dependence of the analyses are addressed.

The systematic uncertainties on the track-reconstruction efficiency depend on the candidate p_T and number of decay tracks of the candidate, and range from 3% to 5% for the D^0, and from 4% to 8% for the D_s^+ and Λ_c^+. The contribution due to the PID was investigated by varying the selection criteria. For the D^0 and the $\Lambda_c^+ \to pK^-\pi^+$ analyses, the studies were performed as described in Refs. [11] and [13], respectively, resulting in a negligible uncertainty for the D^0, and a 5% uncertainty for the $\Lambda_c^+ \to pK^-\pi^+$. In the D_s^+ and $\Lambda_c^+ \to pK_S^0$ analyses, where topological and PID selection variables are used simultaneously in the BDT, the two sources of systematic uncertainty are treated in a combined procedure as described further below.

The possible differences between the real and simulated charm-hadron p_T spectra result in a further source of systematic uncertainty. It was evaluated by reweighting the p_T shape from PYTHIA Monash for the D^0 and D_s^+ analyses and from PYTHIA CR-BLC for the Λ_c^+ analyses to match the one from D-meson FONLL calculations [5, 6]. This contribution ranges from 1% to 6% for $p_T < 4$ GeV/c, while it is negligible at higher p_T.

The selection efficiencies of the various hadron candidates rely on the description of the detector resolution and alignment in the simulation. Systematic effects arising from imperfections in the simulation are studied by repeating the D^0 and $\Lambda_c^+ \to pK^-\pi^+$ analyses using different selection criteria on the displaced decay topology. In the D_s^+ and $\Lambda_c^+ \to pK_S^0$ analyses, the selections on the BDT outputs were varied instead, covering both the PID and the decay-topology selection efficiency. For both approaches, the variations are performed separately for the different multiplicity and p_T intervals. The assigned systematic uncertainties are larger at low p_T where the selection criteria are strict, reaching 5% for the D^0 meson and 10% for the D_s^+ and Λ_c^+ analyses. The uncertainty due to the multiplicity dependence of the selection efficiency was evaluated as well, by changing the weight functions used to reproduce the measured charged-particle multiplicity in the simulation [52]. A maximum deviation of about 4% is observed at low p_T and low multiplicity.

The systematic uncertainty on the raw-yield extraction was evaluated in each combination of the studied p_T and multiplicity intervals by repeating the fit to the invariant-mass distributions varying the fit range and the background fit function as done in Ref. [11]. In order to test the sensitivity to the functional form of the fit function of the signal, the same strategy was performed using a bin-counting method, in which the signal yield was obtained from integrating the background-subtracted invariant-mass distribution. This systematic uncertainty ranges between 2% and 14% depending on the hadron species, the p_T, and the multiplicity interval.

As described above, a data-driven event reweighting procedure was applied for the HMSPD triggered data sample to account for the trigger inefficiency. Three strategies were explored to ensure normalised weights as outlined in Ref. [42]. The different normalisation procedures were propagated to the raw yield calculation resulting in a relative systematic difference of 1% to 4% compared to the central values depending on the particle species, independent of their p_T.

Possible differences between the primary-vertex position distributions along the beam axis, z_{vtx}, in simulations and in data were investigated, since a slight dependence of the efficiencies with z_{vtx} is observed. Hence, a further data-driven reweighting procedure was performed, taking this effect into account. A p_T-dependent systematic uncertainty was estimated, resulting in a contribution of about 0.5% for $p_T < 4$ GeV/c, and negligible elsewhere. This systematic source is considered particle dependent because the weights are defined by selecting events with a charm-hadron candidate in a given invariant-mass range, for each hadron independently.

Systematic effects due to the dependence of the efficiency on the N_{trkl} interval limits were also studied.

These effects were a consequence of removing the reconstructed candidate's decay tracks from the multiplicity in data but not in MC, which was done as the efficiencies have little dependence on multiplicity. The systematic uncertainty was evaluated by comparing the efficiency computed in a N_{trkl} interval shifted by one or two units (for two- or three-body decays, respectively) with the one in the default intervals. It was observed to range from 2% to 8%, especially affecting the lowest p_T and multiplicity interval.

Two systematic uncertainties were assigned to the prompt fraction calculations, coming from the FONLL calculations of the b-quark production [5, 6] and the assumed multiplicity independence of the f_{prompt} factor. The FONLL parameters (b-quark mass, factorisation, and renormalisation scales) were varied as prescribed in Ref. [6]. The assigned uncertainty values for the D mesons range from 3% to 12%. In the Λ_c^+ analyses, the additional contribution from the $f_{b \to \Lambda_b^0}$ fragmentation fraction is considered, as discussed in detail in Ref. [13]. It leads to more asymmetrical values of the uncertainty, ranging from $^{+2}_{-4}$% at low p_T to $^{+6}_{-8}$% at high p_T. As mentioned above, Eq. 1 describes the corrected prompt yields under the assumption that f_{prompt} does not vary with multiplicity. To estimate the uncertainty related to this assumption, PYTHIA simulations where employed, with Monash and CR-BLC tunes. The feed-down contribution from beauty-hadron decays, $f_{feed\text{-}down} = 1 - f_{prompt}$, was varied in each multiplicity interval based on the observed $f_{feed\text{-}down}^{mult}/\langle f_{feed\text{-}down} \rangle$ trends in simulations. The feed-down contributions were found to be compatible for the D and Λ_c^+ hadrons and show a global increasing trend from 0.7 to 1.5 from the lowest to the highest multiplicity event class. The resulting systematic uncertainties depend on the charm-hadron species, the p_T interval, and the multiplicity classes considered in the analyses. For the part related to the f_{prompt} multiplicity-dependence assumption, typical values for the uncertainty for intermediate p_T are $^{+8}_{-0}$% at low multiplicity and $^{+0}_{-15}$% at high multiplicity.

The statistical uncertainty on the selection efficiency is assigned as systematic uncertainty. It strongly depends on the p_T and multiplicity intervals, especially affecting the $p_T < 4$ GeV/c and highest multiplicity intervals, where it reaches 1% for the D^0, 4% for the D_s^+ and $\Lambda_c^+ \to pK^-\pi^+$, and 5% for the $\Lambda_c^+ \to pK_S^0$ analysis. Finally, an overall normalisation systematic uncertainty induced by the branching ratios [47] was considered.

The sources of systematic uncertainty described above are assumed to be uncorrelated among each other and the total systematic uncertainty in each p_T and multiplicity interval is calculated as the quadratic sum of the estimated values. Depending on the p_T and multiplicity intervals, the resulting values range from 7% to 13% for the D^0, from 10% to 17% for the D_s^+, from 7% to 24% for the $\Lambda_c^+ \to pK^-\pi^+$, and from 8% to 17% for the $\Lambda_c^+ \to pK_S^0$ analyses.

5 Results

The p_T-differential corrected yield of the Λ_c^+ baryon was obtained in the different event-multiplicity classes, averaging the results from the two decay channels $\Lambda_c^+ \to pK^-\pi^+$ and $\Lambda_c^+ \to pK_S^0$ to obtain a more precise measurement, for which the inverse of the quadratic sum of the relative statistical and uncorrelated systematic uncertainties were used as weights. In the propagation of the uncertainties, the correlation between the statistical and systematic uncertainties was taken into account, with the strategy explained in Ref. [13]. In addition, the multiplicity-dependent systematic sources were considered as correlated between the two decay channels. In the rest of this section, Λ_c^+ will refer to the weighted average of the $\Lambda_c^+ \to pK^-\pi^+$ and $\Lambda_c^+ \to pK_S^0$ decay channels.

The p_T-differential spectra of D^0, D_s^+, and Λ_c^+ hadrons, measured in $|y| < 0.5$, are shown in Fig. 1 for the INEL > 0 class and the four multiplicity classes selected using the N_{trkl} estimator at midrapidity. The statistical and total systematic uncertainties are shown by vertical error bars and boxes, respectively, as for all the figures in this section. The p_T spectra of the individual decay channels $\Lambda_c^+ \to pK^-\pi^+$ and $\Lambda_c^+ \to pK_S^0$, as well as the D^0, D_s^+, and Λ_c^+ yields in the multiplicity classes selected using the p_{V0M} estimator at forward rapidity, are reported in Ref. [50]. The bottom panels of Fig. 1 present the
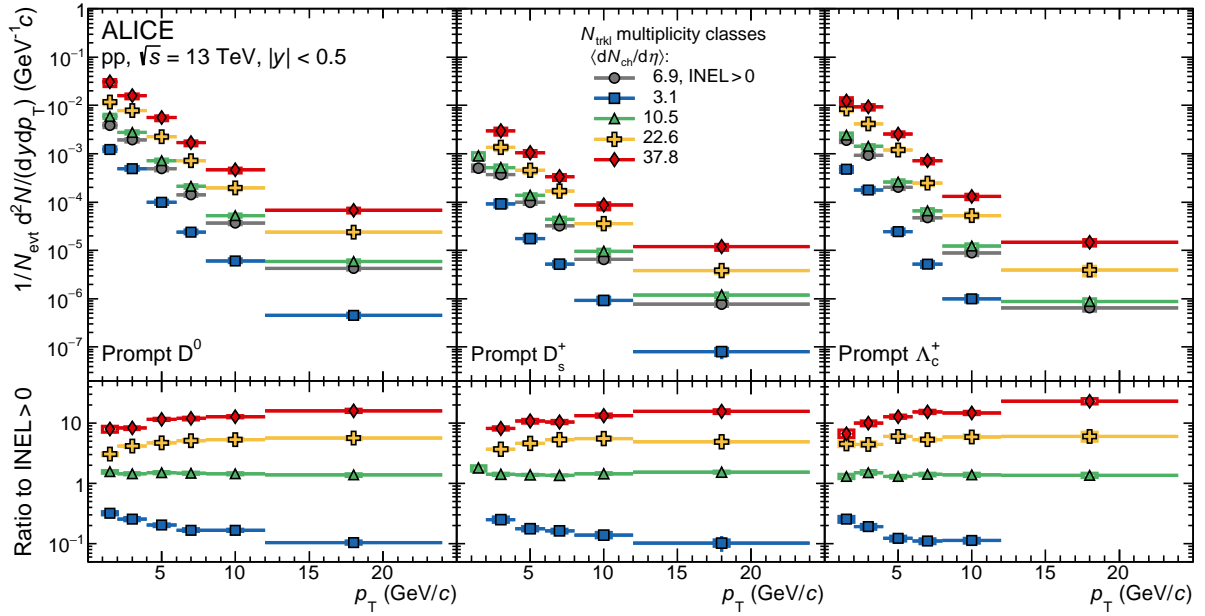
Figure 1: Transverse-momentum spectra of D^0, D_s^+, and Λ_c^+ hadrons measured in pp collisions at $\sqrt{s} = 13$ TeV for different multiplicity classes selected with the N_{trkl} estimator at midrapidity. The corresponding ratios to INEL > 0 are shown in the bottom panels.

ratios to the INEL > 0 class, for which the multiplicity-dependent systematic sources were considered as uncorrelated among different multiplicity classes and the contributions of the tracking and PID efficiency, the shape of MC p_T spectra and z_{vtx} distribution, the beauty feed-down, and the branching ratio as correlated. The statistical uncertainties and the systematic uncertainties related to the selection efficiency and to the raw-yield extraction were considered partially correlated with respect to the measurement performed in the INEL > 0 class.

The measured p_T-differential yields increase from the lowest to the highest multiplicity class for the three hadron species. Their ratios to INEL > 0 increase (decrease) with increasing p_T for the highest (lowest) multiplicity class, suggesting a plateau towards $p_T > 10$ GeV/c, as recently observed for the light-flavour hadrons in Refs. [39, 53, 54], where it was explained as a hardening of the measured p_T spectra with increasing $\langle dN_{ch}/d\eta \rangle$. The effect was shown to be more pronounced for protons than for kaons and pions, and similar for strange baryons and mesons.

In order to investigate potential differences in the $\langle dN_{ch}/d\eta \rangle$ dependence of the D^0-meson production with respect to the D_s^+ meson and Λ_c^+ baryon, the D_s^+/D^0 and Λ_c^+/D^0 yield ratios are compared in different multiplicity event classes in Fig. 2, considering both forward and midrapidity multiplicity estimators. The sources of uncertainty assumed to be uncorrelated between different charm-hadron species included the raw-yield extraction, the selection efficiency, the shape of the MC p_T spectra, the z_{vtx} distribution, and the branching ratio. The systematic uncertainty deriving from the variation of the multiplicity-interval limits was propagated as partially correlated, while the other systematic uncertainties were assumed to be fully correlated.

Within the current experimental uncertainties, the D_s^+/D^0 ratios are independent of p_T in the measured p_T range and compatible with the average of the p_T-integrated results from experiments at e^+e^- and e^-p colliders, 0.17 ± 0.03 [17, 55]. A dependence of these ratios with multiplicity, as seen for the ratio of (multi-)strange hadrons to $\pi^\pm$ [39, 56], is not observed within the uncertainties.

The p_T-differential Λ_c^+/D^0 ratios show an evident dependence on multiplicity, and a hierarchy is ob-
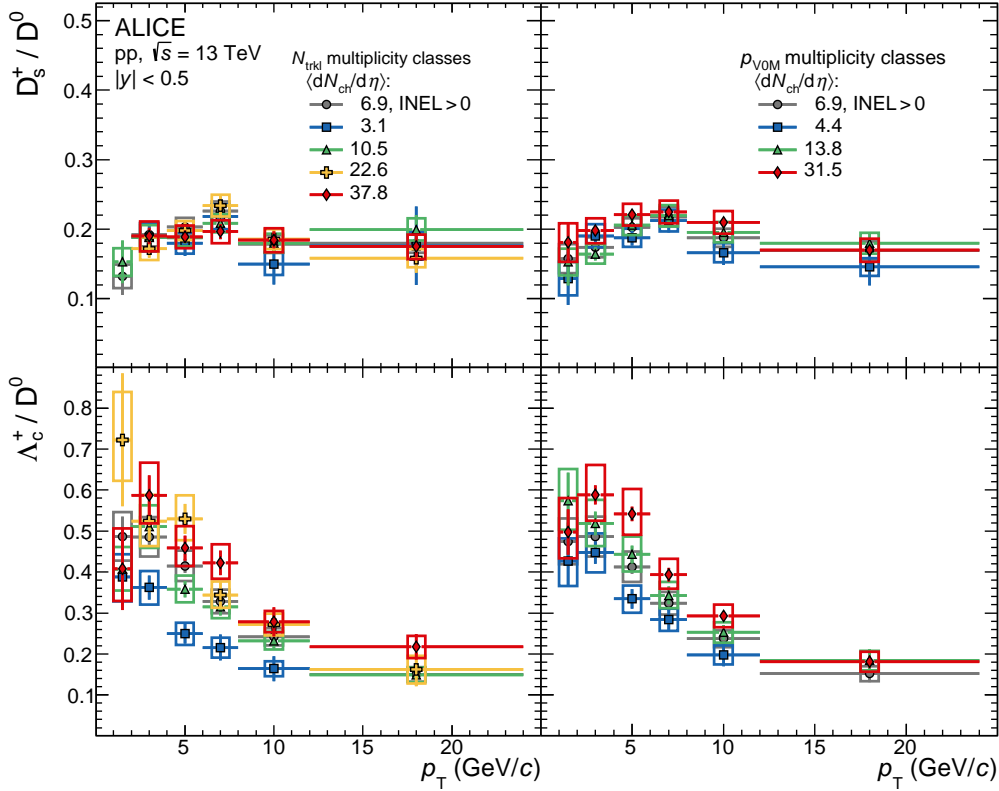
Figure 2: The D_s^+/D^0 (top) and Λ_c^+/D^0 (bottom) ratios measured in pp collisions at $\sqrt{s} = 13$ TeV for different multiplicity classes at mid- (left) and forward (right) rapidity.

served going from the lowest to the highest multiplicity intervals, for both the N_{trkl} and p_{V0M} estimators, for all but the first p_T bin. The increasing trend with $\langle dN_{ch}/d\eta \rangle$ for the Λ_c^+/D^0 ratio is consistent among the measurements done with the two multiplicity estimators, indicating that the enhancement between low and high multiplicity intervals is not a consequence of a possible bias arising from the coinciding rapidity regions between the multiplicity estimator and the measurement of interest at midrapidity. It is worth noticing that the measured Λ_c^+/D^0 ratio in the lowest multiplicity class is still higher, in the measured p_T range, than the average of corresponding ratios measured in e^+e^- collisions at LEP, which was found to be $0.113 \pm 0.013(\text{stat}) \pm 0.006(\text{syst})$ [13, 17].

In order to estimate a significance level for the difference observed in the two extreme multiplicity classes at midrapidity, the highest multiplicity (HM) over the lowest multiplicity (LM) Λ_c^+/D^0 ratio was computed. The probability of the measured double-ratio $DR = (\Lambda_c^+/D^0)_{HM}/(\Lambda_c^+/D^0)_{LM} > 1$, corresponds to a significance of 5.3σ in the $1 < p_T < 12$ GeV/c interval, considering as null hypothesis $DR = 1$. This estimate was performed taking into account statistical and systematic uncertainties, for which the raw-yield extraction, the selection efficiency, the shape of the MC p_T spectra, and the z_{vtx} distribution sources were considered as uncorrelated, the multiplicity-interval limits as partially correlated, while the other sources cancelled out in the double ratio. With the aim of investigating the least favourable case, the measured values in all p_T intervals were shifted down by one standard deviation, by considering the sources of systematic uncertainties correlated with p_T that do not cancel out in the double ratio, i.e. those arising from the selection efficiency and the generated p_T spectra.

The measured charm-hadron ratios for the lowest and highest multiplicity class for the N_{trkl} multiplicity estimator are compared to model predictions from MC generators and a statistical hadronisation model in Fig. 3. The simulations with the PYTHIA event generator were performed with the Monash and the CR-
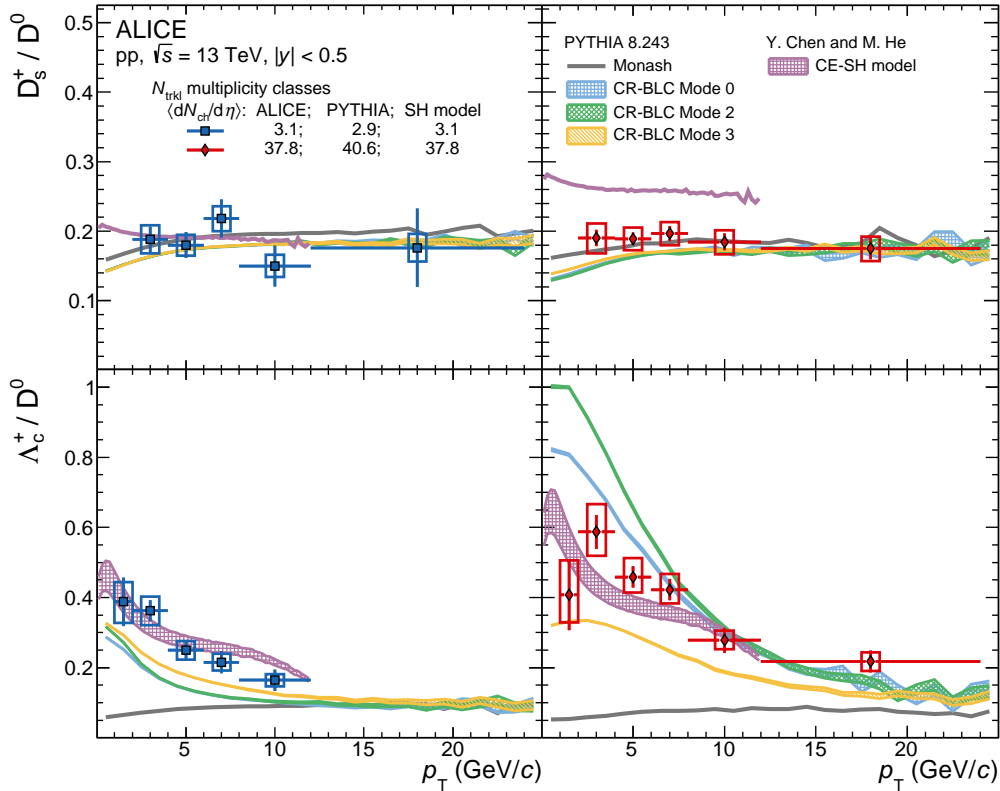
Figure 3: The D_s^+/D^0 (top) and Λ_c^+/D^0 (bottom) ratios measured in pp collisions at $\sqrt{s} = 13$ TeV for the lowest (left) and highest (right) multiplicity classes at midrapidity. The measurements are compared to PYTHIA predictions with the Monash [20] and the CR-BLC tunes [22], and the CE-SH model [57], estimated in similar multiplicity classes. The uncertainty bands for the PYTHIA predictions are the statistical uncertainties on the simulations, while for the CE-SH model they refer to the variation of the branching ratios of the additional charm-baryon states from RQM [58].

BLC tunes. For the latter, three modes are suggested by the authors, applying different constraints on the allowed reconnections among colour sources, in particular concerning the causality connection among strings involved in a reconnection, and time dilation caused by relative boosts of the strings [22]. The simulations are shown in intervals of primary particle multiplicities selected at midrapidity, evaluated by studying the correlation between N_{trkl} intervals and N_{ch} values. The estimated intervals are $1 \leq N_{\text{ch}} \leq 12$ and $N_{\text{ch}} > 75$ for the lowest and highest multiplicity event classes, respectively. The measured D_s^+/D^0 ratios at low and high multiplicity are compatible with PYTHIA with Monash and CR-BLC tunes. The Monash tune, however, does not reproduce the Λ_c^+/D^0 ratio, and furthermore it does not show a multiplicity dependence. By contrast, the CR-BLC tunes describe the Λ_c^+/D^0 decreasing trend with p_{T}, and are closer to the overall magnitude, as also observed for minimum-bias pp collisions at $\sqrt{s} = 5.02$ and 13 TeV [13, 15]. The CR-BLC tunes show a clear dependence with multiplicity, qualitatively reproducing the trend observed in data.

The measurements in Fig. 3 are also compared with the predictions of a canonical-ensemble statistical hadronisation (CE-SH) model [57], where the authors generalise the grand-canonical statistical hadronisation model (SHM) [23] of charm-hadron production to the case of canonical SHM, and explore the multiplicity dependence of charm-hadron particle ratios. The version of the SHM model based on the measured charm-baryon spectrum reported by the PDG [47] was observed to strongly underestimate the Λ_c^+/D^0 measurements in minimum-bias pp collisions [13]. For this reason, for the Λ_c^+/D^0 case, the underlying charm-baryon spectrum in the calculations is augmented to include additional excited baryon

11
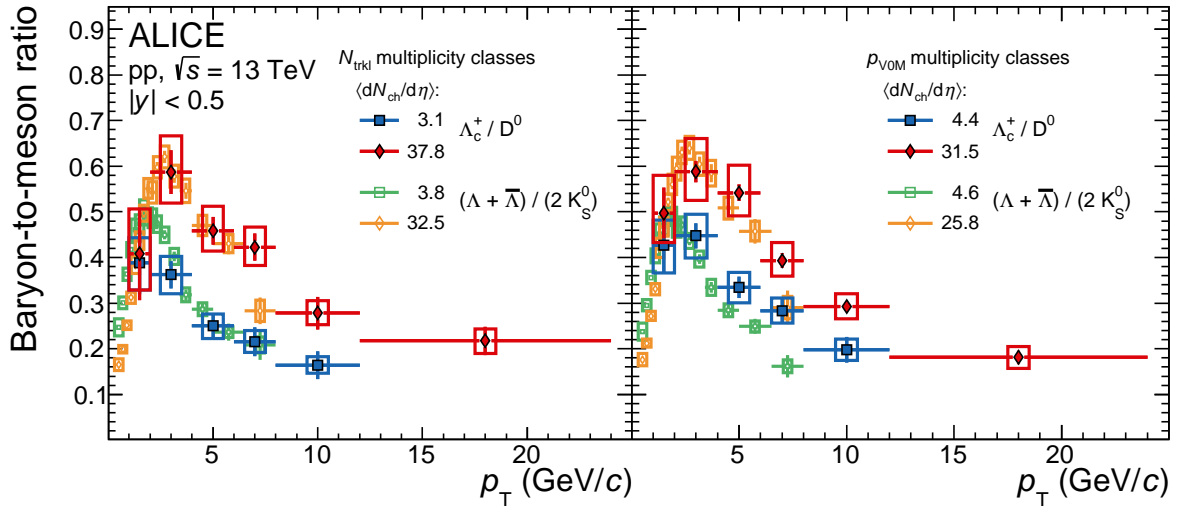
Figure 4: The baryon-to-meson ratios in the light-flavour, based on measurements from Ref. [39] and charm sector measured in pp collisions at $\sqrt{s} = 13$ TeV for similar low- and high-multiplicity classes at mid- (left) and forward (right) rapidity.

states predicted by the Relativistic Quark Model (RQM) [58]. For the D_s^+/D^0 predictions, only the PDG case is shown, since the RQM does not modify the D-meson yields with respect to the PDG set. The model calculations describe the Λ_c^+/D^0 ratios, reproducing the multiplicity dependence. The D_s^+/D^0 prediction is compatible with the measurement for the low multiplicity class, while it overestimates the data in the highest multiplicity interval. The CE-SH model explains the multiplicity dependence as deriving from the reduced volume size of the formalism towards smaller multiplicity, where a decrease of the Λ_c^+/D^0 ratio is a consequence of the strict baryon-number conservation. Such behaviour is also predicted for charm-strange mesons relative to charm mesons, based instead on strangeness-number conservation.

Figure 4 shows the comparison of the Λ_c^+/D^0 and the Λ/K_S^0 [39] baryon-to-meson ratios as a function of p_T in pp collisions at $\sqrt{s} = 13$ TeV, in similar low and high N_{trkl} and p_{V0M} multiplicity classes. In the vacuum-fragmentation scenario, the light-flavour hadron production has a significant contribution from gluon fragmentation, whereas heavy-flavour hadrons are primarily produced through the fragmentation of a charm quark, which is in turn produced in the initial hard scattering. In addition, at low p_T, light-flavour hadrons originate mainly from small-momentum soft scattering processes. Despite these differences, the light- and heavy-flavour baryon-to-meson ratios, Λ_c^+/D^0 and Λ/K_S^0, show a remarkably similar trend as a function of $\langle dN_{\text{ch}}/d\eta \rangle$. The measurements also suggest a similar shift of the baryon-to-meson ratio peaks towards higher momenta, with increasing multiplicity. These similarities, observed as well in minimum-bias pp and p–Pb collisions at $\sqrt{s_{\text{NN}}} = 5.02$ TeV both in terms of shape and magnitude [59], hint at a potential common mechanism for light- and charm-baryon formation in hadronic collisions at LHC energies.

The p_T-integrated yields of Λ_c^+ and D^0 were computed by integrating the p_T-differential spectra in their measured range and extrapolating them down to $p_T = 0$ in each multiplicity interval. In the integration, the systematic uncertainties were propagated considering the uncertainty due to the raw-yield extraction and the statistical uncertainty on the efficiency as fully uncorrelated and all the other sources as fully correlated among p_T intervals. The PYTHIA predictions with CR-BLC Mode 2 were used for the extrapolation in each multiplicity interval, for both Λ_c^+ and D^0, following a similar procedure as the one described in Ref. [13]. The extrapolation factor was computed as the ratio of the PYTHIA spectrum integrated in the full p_T range to the integral in the visible p_T range. The Λ_c^+ and D^0 yields in the full p_T range were obtained by integrating the yield in the visible p_T interval and scaling by the extrapo-
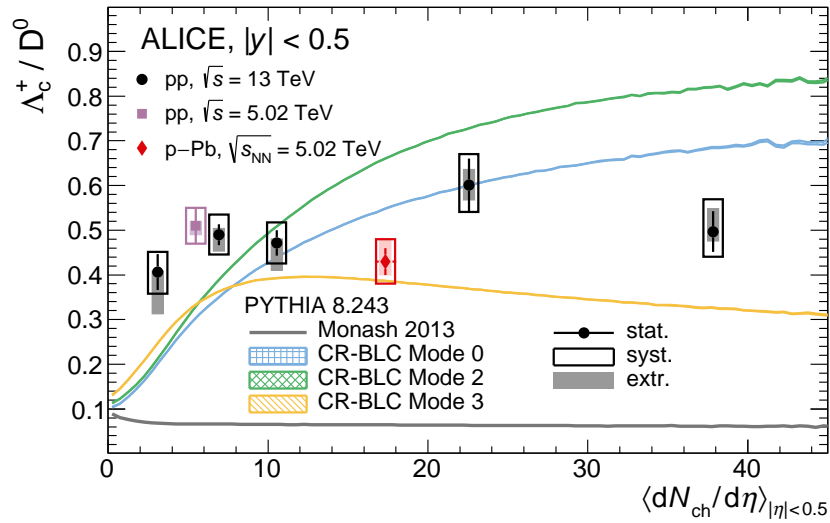
Figure 5: Ratios of p_{T}-integrated yields of Λ_c^+ and D^0 hadrons as a function of $\langle dN_{ch}/d\eta \rangle$ in pp collisions at $\sqrt{s} = 13$ TeV. Measurements performed in pp and p–Pb collisions at $\sqrt{s_{NN}} = 5.02$ TeV from Ref. [13] are also shown. Statistical and systematic uncertainties are shown by error bars and empty boxes, respectively. Shaded boxes represent the extrapolation uncertainties. The corresponding PYTHIA predictions [20, 22] are also shown.

lation factor. The fraction of extrapolated yield from the lowest to the highest multiplicity interval is about 39% (31%), 28% (22%), 20% (16%), and 15% (13%) for Λ_c^+ (D^0). The procedure was repeated considering also the CR-BLC Mode 0 and Mode 3 as well as two different functions fitted to the spectra (a Tsallis-Lévy [60] and a power-law function). The fits were performed considering the statistical and p_{T}-uncorrelated sources of systematic uncertainties, and also shifting up and down the data by one sigma of the p_{T}-correlated systematic uncertainties. The envelope of the extrapolation factors obtained with all the trials was assigned as the extrapolation uncertainty on Λ_c^+ and D^0, and it was propagated to the Λ_c^+/D^0 ratio, resulting in a value that ranges from 2% to 21% depending on multiplicity. The same procedure was used to estimate the p_{T}-integrated D_s^+ yields and D_s^+/D^0 yield ratios in the different multiplicity intervals, reported in Ref. [50]. The Λ_c^+ and D^0 p_{T}-integrated yields are also reported in Ref. [50], together with the p_{T}-integrated Λ_c^+/D^0 yield ratios in the visible p_{T} range, and the tables with the numerical values of the p_{T}-integrated ratios. The p_{T}-integrated Λ_c^+/D^0 yield ratio as a function of $\langle dN_{ch}/d\eta \rangle$ is shown in Fig. 5, where the systematic uncertainties from the extrapolation (shaded boxes, assumed to be uncorrelated among multiplicity intervals) are drawn separately from the other sources of systematic uncertainties (empty boxes). The sources related to the raw-yield extraction, the multiplicity-interval limits, the high-multiplicity triggers, the multiplicity-independent prompt fraction assumption, and the statistical uncertainties on the efficiencies are also considered uncorrelated with multiplicity. The other systematic uncertainties are assumed to be correlated. The measurements performed in pp and p–Pb collisions at $\sqrt{s} = 5.02$ TeV [13] are also shown. The result does not favour an increase of the yield ratios with multiplicity, as also observed for the Λ/K_S^0 ratio in Ref. [39], and the trend is compatible with a constant function. This suggests that the increasing trend observed for the $1 < p_{\mathrm{T}} < 24$ GeV/c range comes from a re-distribution of p_{T} that acts differently for baryons and mesons, while this is not observed in the meson-to-meson ratios, as shown in Fig. 3 for D_s^+/D^0 and in Ref. [54] for K/π. The results are compared to the p_{T}-integrated PYTHIA predictions. The measurements exclude the Monash prediction in the whole multiplicity range, and tend to be significantly below the CR-BLC Mode 2 for the three highest multiplicity intervals.

13

6   Conclusions

The first measurement of D_s^+/D^0 and Λ_c^+/D^0 ratios as a function of charged-particle multiplicity in pp collisions at $\sqrt{s} = 13$ TeV was presented. The p_T-differential D_s^+/D^0 yield ratio does not show a dependence on multiplicity, within uncertainties. In contrast, the charm baryon-to-meson ratio, Λ_c^+/D^0, measured as a function of p_T, shows a significant increase (5.3σ) when comparing the measurements performed in the lowest and highest multiplicity intervals in $1 < p_T < 12$ GeV/c. In addition, the Λ_c^+/D^0 ratio measured in the lowest multiplicity interval ($\langle dN_{ch}/d\eta \rangle = 3.1$) is higher, at low and intermediate p_T, than the values measured at e^+e^- colliders at lower centre-of-mass energies. These observations imply a modification of the hadronisation mechanisms that is collision-system and multiplicity dependent, further confirming the limited validity of the assumption of universality of the fragmentation functions. The measurements are compared with two calculations. Those based on PYTHIA with CR-BLC describe the D_s^+/D^0 measurements and capture the trend of the Λ_c^+/D^0 ratio, qualitatively describing the increasing magnitude of the baryon-to-meson ratios with multiplicity. Calculations based on a statistical hadronisation model, with the multiplicity dependence originating from the canonical treatment of quantum-charge conservation, describe the Λ_c^+/D^0 measurements in the lowest and highest multiplicity intervals. The prediction is also in agreement with the D_s^+/D^0 ratio for the low multiplicity interval, while it overestimates the data in the high-multiplicity class. The baryon-to-meson ratios in the charm sector, Λ_c^+/D^0, are also compared to those in the light-flavour sector, Λ/K_S^0, in similar multiplicity classes, showing a remarkably similar trend as a function of p_T and similar enhancement with $\langle dN_{ch}/d\eta \rangle$. These similarities hint at a possible common mechanism for light- and charm-baryon formation in pp collisions at LHC energies. The p_T-integrated Λ_c^+/D^0 ratios, extrapolated to $p_T = 0$ based on spectral shapes from PYTHIA with CR-BLC, show no significant dependence on multiplicity, suggesting that the increase in the baryon-to-meson yield ratio observed in the measured p_T range is due to a different redistribution of p_T between baryons and mesons, rather than to an enhancement in the overall baryon yield. More precise measurements with the data sample collected in Run 3 of the LHC will allow us to further investigate the shape of the p_T-integrated baryon-to-meson ratios versus multiplicity, extending the multiplicity reach to lower and higher multiplicity intervals.

References

[1] J. C. Collins, D. E. Soper, and G. F. Sterman, "Factorization of Hard Processes in QCD", *Adv. Ser. Direct. High Energy Phys.* **5** (1989) 1–91, `arXiv:hep-ph/0409313`.

[2] E. Braaten, K.-M. Cheung, S. Fleming, and T. C. Yuan, "Perturbative QCD fragmentation functions as a model for heavy quark fragmentation", *Phys. Rev. D* **51** (1995) 4819–4829, `arXiv:hep-ph/9409316`.

[3] B. A. Kniehl, G. Kramer, I. Schienbein, and H. Spiesberger, "Collinear subtractions in hadroproduction of heavy quarks", *Eur. Phys. J.* **C41** (2005) 199–212, `arXiv:hep-ph/0502194 [hep-ph]`.

[4] B. A. Kniehl, G. Kramer, I. Schienbein, and H. Spiesberger, "Inclusive Charmed-Meson Production at the CERN LHC", *Eur. Phys. J.* **C72** (2012) 2082, `arXiv:1202.0439 [hep-ph]`.

[5] M. Cacciari, M. Greco, and P. Nason, "The p_T Spectrum in Heavy-Flavour Hadroproduction", *JHEP* **05** (1998) 007, `arXiv:hep-ph/9803400 [hep-ph]`.

[6] M. Cacciari *et al.*, "Theoretical predictions for charm and bottom production at the LHC", *JHEP* **10** (2012) 137, `arXiv:1205.6344 [hep-ph]`.

[7] A. Andronic *et al.*, "Heavy-flavour and quarkonium production in the LHC era: from proton–proton to heavy-ion collisions", *Eur. Phys. J.* **C76** no. 3, (2016) 107, arXiv:1506.03981 [nucl-ex].

[8] **LHCb** Collaboration, R. Aaij *et al.*, "Measurements of prompt charm production cross-sections in pp collisions at $\sqrt{s} = 13$ TeV", *JHEP* **03** (2016) 159, arXiv:1510.01707 [hep-ex]. [Erratum: *JHEP* **09** (2016), 013; Erratum: *JHEP* **05** (2017), 074].

[9] **CMS** Collaboration, V. Khachatryan *et al.*, "Measurement of the total and differential inclusive B^+ hadron cross sections in pp collisions at $\sqrt{s} = 13$ TeV", *Phys. Lett.* **B771** (2017) 435–456, arXiv:1609.00873 [hep-ex].

[10] **LHCb** Collaboration, R. Aaij *et al.*, "Measurement of the $B^\pm$ production cross-section in pp collisions at $\sqrt{s} = 7$ and 13 TeV", *JHEP* **12** (2017) 026, arXiv:1710.04921 [hep-ex].

[11] **ALICE** Collaboration, S. Acharya *et al.*, "Measurement of D^0, D^+, D^{*+} and D_s^+ production in pp collisions at $\sqrt{s} = 5.02$ TeV with ALICE", *Eur. Phys. J.* **C79** no. 5, (2019) 388, arXiv:1901.07979 [nucl-ex].

[12] **ALICE** Collaboration, S. Acharya *et al.*, "Λ_c^+ production in pp collisions at $\sqrt{s} = 7$ TeV and in p–Pb collisions at $\sqrt{s_{\mathrm{NN}}} = 5.02$ TeV", *JHEP* **04** (2018) 108, arXiv:1712.09581 [nucl-ex].

[13] **ALICE** Collaboration, S. Acharya *et al.*, "Λ_c^+ production in pp and in p–Pb collisions at $\sqrt{s_{NN}} = 5.02$ TeV", *Phys. Rev. C* **104** (2021) 054905, arXiv:2011.06079 [nucl-ex].

[14] **CMS** Collaboration, A. M. Sirunyan *et al.*, "Production of Λ_c^+ baryons in proton–proton and lead–lead collisions at $\sqrt{s_{\mathrm{NN}}} = 5.02$ TeV", *Phys. Lett. B* **803** (2020) 135328, arXiv:1906.03322 [hep-ex].

[15] **ALICE** Collaboration, S. Acharya *et al.*, "Measurement of prompt D^0, Λ_c^+, and $\Sigma_c^{0,++}(2455)$ production in pp collisions at $\sqrt{s} = 13$ TeV", arXiv:2106.08278 [hep-ex].

[16] B. A. Kniehl, G. Kramer, I. Schienbein, and H. Spiesberger, "$\Lambda_c^\pm$ production in pp collisions with a new fragmentation function", *Phys. Rev. D* **101** no. 11, (2020) 114021, arXiv:2004.04213 [hep-ph].

[17] L. Gladilin, "Fragmentation fractions of c and b quarks into charmed hadrons at LEP", *Eur. Phys. J. C* **75** no. 1, (2015) 19, arXiv:1404.3888 [hep-ex].

[18] **LHCb** Collaboration, R. Aaij *et al.*, "Prompt Λ_c^+ production in p–Pb collisions at $\sqrt{s_{\mathrm{NN}}} = 5.02$ TeV", *JHEP* **02** (2019) 102, arXiv:1809.01404 [hep-ex].

[19] T. Sjöstrand *et al.*, "An introduction to PYTHIA 8.2", *Comput. Phys. Commun.* **191** (2015) 159–177, arXiv:1410.3012 [hep-ph].

[20] P. Skands, S. Carrazza, and J. Rojo, "Tuning PYTHIA 8.1: the Monash 2013 Tune", *Eur. Phys. J.* **C74** no. 8, (2014) 3024, arXiv:1404.5630 [hep-ph].

[21] J. Bellm *et al.*, "Herwig 7.0/Herwig++ 3.0 release note", *Eur. Phys. J. C* **76** no. 4, (2016) 196, arXiv:1512.01178 [hep-ph].

[22] J. R. Christiansen and P. Z. Skands, "String Formation Beyond Leading Colour", *JHEP* **08** (2015) 003, arXiv:1505.01681 [hep-ph].

[23] M. He and R. Rapp, "Charm-baryon production in proton–proton collisions", *Phys. Lett. B* **795** (2019) 117–121, arXiv:1902.08889 [nucl-th].

[24] V. Minissale, S. Plumari, and V. Greco, "Charm Hadrons in pp collisions at LHC energy within a Coalescence plus Fragmentation approach", arXiv:2012.12001 [hep-ph].

[25] **ALICE** Collaboration, S. Acharya *et al.*, "First measurement of Ξ_c^0 production in pp collisions at $\sqrt{s} = 7$ TeV", *Phys. Lett. B* **781** (2018) 8–19, arXiv:1712.04242 [hep-ex].

[26] **ALICE** Collaboration, S. Acharya *et al.*, "Measurement of the production cross section of prompt Ξ_c^0 baryons at midrapidity in pp collisions at $\sqrt{s} = 5.02$ TeV", *JHEP* **10** (2021) 159, arXiv:2105.05616 [nucl-ex].

[27] **ALICE** Collaboration, S. Acharya *et al.*, "Measurement of the cross sections of Ξ_c^0 and Ξ_c^+ baryons and branching-fraction ratio BR($\Xi_c^0 \to \Xi^- e^+ \nu_e$)/BR($\Xi_c^0 \to \Xi^- \pi^+$) in pp collisions at 13 TeV", arXiv:2105.05187 [nucl-ex].

[28] **ALICE** Collaboration, S. Acharya *et al.*, "Charm-quark fragmentation fractions and production cross section at midrapidity in pp collisions at the LHC", arXiv:2105.06335 [nucl-ex].

[29] W. Busza, K. Rajagopal, and W. van der Schee, "Heavy Ion Collisions: The Big Picture, and the Big Questions", *Ann. Rev. Nucl. Part. Sci.* **68** (2018) 339–376, arXiv:1802.04801 [hep-ph].

[30] **ALICE** Collaboration, B. Abelev *et al.*, "K_S^0 and Λ production in Pb–Pb collisions at $\sqrt{s_{NN}} = 2.76$ TeV", *Phys. Rev. Lett.* **111** (2013) 222301, arXiv:1307.5530 [nucl-ex].

[31] **STAR** Collaboration, J. Adams *et al.*, "Measurements of identified particles at intermediate transverse momentum in the STAR experiment from Au + Au collisions at $\sqrt{s_{NN}} = 200$ GeV", arXiv:nucl-ex/0601042.

[32] **ALICE** Collaboration, S. Acharya *et al.*, "Λ_c^+ production in Pb–Pb collisions at $\sqrt{s_{NN}} = 5.02$ TeV", *Phys. Lett.* **B793** (2019) 212–223, arXiv:1809.10922 [nucl-ex].

[33] **STAR** Collaboration, J. Adam *et al.*, "Observation of enhancement of charmed baryon-to-meson ratio in Au+Au collisions at $\sqrt{s_{NN}} = 200$ GeV", *Phys. Rev. Lett.* **124** no. 17, (2020) 172301, arXiv:1910.14628 [nucl-ex].

[34] **ALICE** Collaboration, S. Acharya *et al.*, "Prompt D^0, D^+, and D^{*+} production in Pb-Pb collisions at $\sqrt{s_{NN}} = 5.02$ TeV", arXiv:2110.09420 [nucl-ex].

[35] **ALICE** Collaboration, S. Acharya *et al.*, "Measurement of D^0, D^+, D^{*+} and D_s^+ production in Pb–Pb collisions at $\sqrt{s_{NN}} = 5.02$ TeV", *JHEP* **10** (2018) 174, arXiv:1804.09083 [nucl-ex].

[36] **ALICE** Collaboration, S. Acharya *et al.*, "Measurement of prompt D_s^+-meson production and azimuthal anisotropy in Pb-Pb collisions at $\sqrt{s_{NN}} = 5.02$ TeV", arXiv:2110.10006 [nucl-ex].

[37] **STAR** Collaboration, J. Adam *et al.*, "Observation of $D_s^\pm / D^0$ enhancement in Au+Au collisions at $\sqrt{s_{NN}} = 200$ GeV", *Phys. Rev. Lett.* **127** (2021) 092301, arXiv:2101.11793 [hep-ex].

[38] R. J. Fries, V. Greco, and P. Sorensen, "Coalescence Models For Hadron Formation From Quark Gluon Plasma", *Ann. Rev. Nucl. Part. Sci.* **58** (2008) 177–205, arXiv:0807.4939 [nucl-th].

[39] **ALICE** Collaboration, S. Acharya *et al.*, "Multiplicity dependence of (multi-)strange hadron production in proton–proton collisions at $\sqrt{s} = 13$ TeV", *Eur. Phys. J. C* **80** no. 2, (2020) 167, arXiv:1908.01861 [nucl-ex].

[40] **ALICE** Collaboration, K. Aamodt *et al.*, "The ALICE experiment at the CERN LHC", *JINST* **3** (2008) S08002.

[41] **ALICE** Collaboration, B. Abelev *et al.*, "Performance of the ALICE Experiment at the CERN LHC", *Int. J. Mod. Phys. A* **29** (2014) 1430044, arXiv:1402.4476 [nucl-ex].

[42] **ALICE** Collaboration, J. Adam *et al.*, "Measurement of charm and beauty production at central rapidity versus charged-particle multiplicity in proton–proton collisions at $\sqrt{s} = 7$ TeV", *JHEP* **09** (2015) 148, arXiv:1505.00664 [nucl-ex].

[43] **ALICE** Collaboration, S. Acharya *et al.*, "Pseudorapidity distributions of charged particles as a function of mid- and forward rapidity multiplicities in pp collisions at $\sqrt{s} = 5.02$, 7 and 13 TeV", *Eur. Phys. J. C* **81** no. 7, (2021) 630, arXiv:2009.09434 [nucl-ex].

[44] **ALICE** Collaboration, J. Adam *et al.*, "Charged-particle multiplicities in proton–proton collisions at $\sqrt{s} = 0.9$ to 8 TeV", *Eur. Phys. J. C* **77** no. 1, (2017) 33, arXiv:1509.07541 [nucl-ex].

[45] **ALICE** Collaboration, S. Acharya *et al.*, "The ALICE definition of primary particles", ALICE-PUBLIC-2017-005. https://cds.cern.ch/record/2270008.

[46] R. Brun *et al.*, "GEANT: Detector Description and Simulation Tool", CERN-W-5013. http://cds.cern.ch/record/1082634.

[47] **Particle Data Group** Collaboration, P. Zyla *et al.*, "Review of Particle Physics", *PTEP* **2020** no. 8, (2020) 083C01.

[48] T. Chen and C. Guestrin, "XGBoost: A Scalable Tree Boosting System", *Proceedings of the 22nd ACM SIGKDD International Conference on Knowledge Discovery and Data Mining* (201 arXiv:1603.02754 [cs.LG].

[49] **ALICE** Collaboration, S. Acharya *et al.*, "Measurement of beauty and charm production in pp collisions at $\sqrt{s} = 5.02$ TeV via non-prompt and prompt D mesons", *JHEP* **05** (2021) 220, arXiv:2102.13601 [nucl-ex].

[50] **ALICE** Collaboration, S. Acharya *et al.*, "Supplemental material: Observation of a multiplicity dependence in the p_T-differential charm baryon-to-meson ratios in proton–proton collisions at $\sqrt{s} = 13$ TeV",. http://cds.cern.ch/record/2791263.

[51] **LHCb** Collaboration, R. Aaij *et al.*, "Measurement of *b* hadron fractions in 13 TeV pp collisions", *Phys. Rev. D* **100** no. 3, (2019) 031102, arXiv:1902.06794 [hep-ex].

[52] **ALICE** Collaboration, J. Adam *et al.*, "Measurement of D-meson production versus multiplicity in p–Pb collisions at $\sqrt{s_{NN}} = 5.02$ TeV", *JHEP* **08** (2016) 078, arXiv:1602.07240 [nucl-ex].

[53] **ALICE** Collaboration, S. Acharya *et al.*, "Multiplicity dependence of π, K, and p production in pp collisions at $\sqrt{s} = 13$ TeV", *Eur. Phys. J. C* **80** no. 8, (2020) 693, arXiv:2003.02394 [nucl-ex].

[54] **ALICE** Collaboration, S. Acharya *et al.*, "Multiplicity dependence of light-flavor hadron production in pp collisions at $\sqrt{s} = 7$ TeV", *Phys. Rev. C* **99** no. 2, (2019) 024906, arXiv:1807.11321 [nucl-ex].

[55] M. Lisovyi, A. Verbytskyi, and O. Zenaiev, "Combined analysis of charm-quark fragmentation-fraction measurements", *Eur. Phys. J. C* **76** no. 7, (2016) 397, arXiv:1509.01061 [hep-ex].

[56] **ALICE** Collaboration, J. Adam *et al.*, "Enhanced production of multi-strange hadrons in high-multiplicity proton–proton collisions", *Nature Phys.* **13** (2017) 535–539, arXiv:1606.07424 [nucl-ex].

[57] Y. Chen and M. He, "Charged-particle multiplicity dependence of charm-baryon-to-meson ratio in high-energy proton–proton collisions", *Phys. Lett. B* **815** (2021) 136144, arXiv:2011.14328 [hep-ph].

[58] D. Ebert, R. Faustov, and V. Galkin, "Spectroscopy and Regge trajectories of heavy baryons in the relativistic quark-diquark picture", *Phys. Rev. D* **84** (2011) 014025, arXiv:1105.0583 [hep-ph].

[59] **ALICE** Collaboration, S. Acharya *et al.*, "Λ_c^+ production and Baryon-to-Meson Ratios in pp and p–Pb collisions at $\sqrt{s_{\mathrm{NN}}} = 5.02$ TeV at the LHC", *Phys. Rev. Lett.* **127** (2021) 202301, arXiv:2011.06078 [nucl-ex].

[60] D. Prato and C. Tsallis, "Nonextensive foundation of Levy distributions", *Phys. Rev. E* **60** (1999) 2398.

A   The ALICE Collaboration

S. Acharya[142], D. Adamová[96], A. Adler[74], J. Adolfsson[81], G. Aglieri Rinella[34], M. Agnello[30],
N. Agrawal[54], Z. Ahammed[142], S. Ahmad[16], S.U. Ahn[76], I. Ahuja[38], Z. Akbar[51], A. Akindinov[93],
M. Al-Turany[108], S.N. Alam[16], D. Aleksandrov[89], B. Alessandro[59], H.M. Alfanda[7], R. Alfaro Molina[71],
B. Ali[16], Y. Ali[14], A. Alici[25], N. Alizadehvandchali[125], A. Alkin[34], J. Alme[21], G. Alocco[55], T. Alt[68],
I. Altsybeev[113], M.N. Anaam[7], C. Andrei[48], D. Andreou[91], A. Andronic[145], V. Anguelov[105],
F. Antinori[57], P. Antonioli[54], C. Anuj[16], N. Apadula[80], L. Aphecetche[115], H. Appelshäuser[68],
S. Arcelli[25], R. Arnaldi[59], I.C. Arsene[20], M. Arslandok[147], A. Augustinus[34], R. Averbeck[108], S. Aziz[78],
M.D. Azmi[16], A. Badalà[56], Y.W. Baek[41], X. Bai[129,108], R. Bailhache[68], Y. Bailung[50], R. Bala[102],
A. Balbino[30], A. Baldisseri[139], B. Balis[2], D. Banerjee[4], Z. Banoo[102], R. Barbera[26], L. Barioglio[106],
M. Barlou[85], G.G. Barnaföldi[146], L.S. Barnby[95], V. Barret[136], C. Bartels[128], K. Barth[34], E. Bartsch[68],
F. Baruffaldi[27], N. Bastid[136], S. Basu[81], G. Batigne[115], B. Batyunya[75], D. Bauri[49], J.L. Bazo Alba[112],
I.G. Bearden[90], C. Beattie[147], P. Becht[108], I. Belikov[138], A.D.C. Bell Hechavarria[145], F. Bellini[25],
R. Bellwied[125], S. Belokurova[113], V. Belyaev[94], G. Bencedi[146,69], S. Beole[24], A. Bercuci[48],
Y. Berdnikov[99], A. Berdnikova[105], L. Bergmann[105], M.G. Besoiu[67], L. Betev[34], P.P. Bhaduri[142],
A. Bhasin[102], I.R. Bhat[102], M.A. Bhat[4], B. Bhattacharjee[42], P. Bhattacharya[22], L. Bianchi[24],
N. Bianchi[52], J. Bielčík[37], J. Bielčíková[96], J. Biernat[118], A. Bilandzic[106], G. Biro[146], S. Biswas[4],
J.T. Blair[119], D. Blau[89,82], M.B. Blidaru[108], C. Blume[68], G. Boca[28,58], F. Bock[97], A. Bogdanov[94],
S. Boi[22], J. Bok[61], L. Boldizsár[146], A. Bolozdynya[94], M. Bombara[38], P.M. Bond[34], G. Bonomi[141,58],
H. Borel[139], A. Borissov[82], H. Bossi[147], E. Botta[24], L. Bratrud[68], P. Braun-Munzinger[108],
M. Bregant[121], M. Broz[37], G.E. Bruno[107,33], M.D. Buckland[23,128], D. Budnikov[109], H. Buesching[68],
S. Bufalino[30], O. Bugnon[115], P. Buhler[114], Z. Buthelezi[72,132], J.B. Butt[14], A. Bylinkin[127],
S.A. Bysiak[118], M. Cai[27,7], H. Caines[147], A. Caliva[108], E. Calvo Villar[112], J.M.M. Camacho[120],
R.S. Camacho[45], P. Camerini[23], F.D.M. Canedo[121], F. Carnesecchi[34,25], R. Caron[137,139], J. Castillo
Castellanos[139], E.A.R. Casula[22], F. Catalano[30], C. Ceballos Sanchez[75], I. Chakaberia[80],
P. Chakraborty[49], S. Chandra[142], S. Chapeland[34], M. Chartier[128], S. Chattopadhyay[142],
S. Chattopadhyay[110], T.G. Chavez[45], T. Cheng[7], C. Cheshkov[137], B. Cheynis[137], V. Chibante Barroso[34],
D.D. Chinellato[122], S. Cho[61], P. Chochula[34], P. Christakoglou[91], C.H. Christensen[90], P. Christiansen[81],
T. Chujo[134], C. Cicalo[55], L. Cifarelli[25], F. Cindolo[54], M.R. Ciupek[108], G. Clai[II,54], J. Cleymans[I,124],
F. Colamaria[53], J.S. Colburn[111], D. Colella[53,107,33], A. Collu[80], M. Colocci[34], M. Concas[III,59],
G. Conesa Balbastre[79], Z. Conesa del Valle[78], G. Contin[23], J.G. Contreras[37], M.L. Coquet[139],
T.M. Cormier[97], P. Cortese[31], M.R. Cosentino[123], F. Costa[34], S. Costanza[28,58], P. Crochet[136],
R. Cruz-Torres[80], E. Cuautle[69], P. Cui[7], L. Cunqueiro[97], A. Dainese[57], M.C. Danisch[105], A. Danu[67],
P. Das[87], P. Das[4], S. Das[4], S. Dash[49], A. De Caro[29], G. de Cataldo[53], L. De Cilladi[24], J. de Cuveland[39],
A. De Falco[22], D. De Gruttola[29], N. De Marco[59], C. De Martin[23], S. De Pasquale[29], S. Deb[50],
H.F. Degenhardt[121], K.R. Deja[143], R. Del Grande[106], L. Dello Stritto[29], W. Deng[7], P. Dhankher[19], D. Di
Bari[33], A. Di Mauro[34], R.A. Diaz[8], T. Dietel[124], Y. Ding[137,7], R. Divià[34], D.U. Dixit[19], Ø. Djuvsland[21],
U. Dmitrieva[63], J. Do[61], A. Dobrin[67], B. Dönigus[68], A.K. Dubey[142], A. Dubla[108,91], S. Dudi[101],
P. Dupieux[136], N. Dzalaiova[13], T.M. Eder[145], R.J. Ehlers[97], V.N. Eikeland[21], F. Eisenhut[68], D. Elia[53],
B. Erazmus[115], F. Ercolessi[25], F. Erhardt[100], A. Erokhin[113], M.R. Ersdal[21], B. Espagnon[78], G. Eulisse[34],
D. Evans[111], S. Evdokimov[92], L. Fabbietti[106], M. Faggin[27], J. Faivre[79], F. Fan[7], W. Fan[80], A. Fantoni[52],
M. Fasel[97], P. Fecchio[30], A. Feliciello[59], G. Feofilov[113], A. Fernández Téllez[45], A. Ferrero[139],
A. Ferretti[24], V.J.G. Feuillard[105], J. Figiel[118], V. Filova[37], D. Finogeev[63], F.M. Fionda[55], G. Fiorenza[34],
F. Flor[125], A.N. Flores[119], S. Foertsch[72], S. Fokin[89], E. Fragiacomo[60], E. Frajna[146], A. Francisco[136],
U. Fuchs[34], N. Funicello[29], C. Furget[79], A. Furs[63], J.J. Gaardhøje[90], M. Gagliardi[24], A.M. Gago[112],
A. Gal[138], C.D. Galvan[120], P. Ganoti[85], C. Garabatos[108], J.R.A. Garcia[45], E. Garcia-Solis[10], K. Garg[115],
C. Gargiulo[34], A. Garibli[88], K. Garner[145], P. Gasik[108], E.F. Gauger[119], A. Gautam[127], M.B. Gay
Ducati[70], M. Germain[115], P. Ghosh[142], S.K. Ghosh[4], M. Giacalone[25], P. Gianotti[52], P. Giubellino[108,59],
P. Giubilato[27], A.M.C. Glaenzer[139], P. Glässel[105], E. Glimos[131], D.J.Q. Goh[83], V. Gonzalez[144],

L.H. González-Trueba[71], S. Gorbunov[39], M. Gorgon[2], L. Görlich[118], S. Gotovac[35], V. Grabski[71], L.K. Graczykowski[143], L. Greiner[80], A. Grelli[62], C. Grigoras[34], V. Grigoriev[94], S. Grigoryan[75,1], F. Grosa[34,59], J.F. Grosse-Oetringhaus[34], R. Grosso[108], D. Grund[37], G.G. Guardiano[122], R. Guernane[79], M. Guilbaud[115], K. Gulbrandsen[90], T. Gunji[133], W. Guo[7], A. Gupta[102], R. Gupta[102], S.P. Guzman[45], L. Gyulai[146], M.K. Habib[108], C. Hadjidakis[78], H. Hamagaki[83], M. Hamid[7], R. Hannigan[119], M.R. Haque[143], A. Harlenderova[108], J.W. Harris[147], A. Harton[10], J.A. Hasenbichler[34], H. Hassan[97], D. Hatzifotiadou[54], P. Hauer[43], L.B. Havener[147], S.T. Heckel[106], E. Hellbär[108], H. Helstrup[36], T. Herman[37], E.G. Hernandez[45], G. Herrera Corral[9], F. Herrmann[145], K.F. Hetland[36], H. Hillemanns[34], C. Hills[128], B. Hippolyte[138], B. Hofman[62], B. Hohlweger[91], J. Honermann[145], G.H. Hong[148], D. Horak[37], S. Hornung[108], A. Horzyk[2], R. Hosokawa[15], Y. Hou[7], P. Hristov[34], C. Hughes[131], P. Huhn[68], L.M. Huhta[126], C.V. Hulse[78], T.J. Humanic[98], H. Hushnud[110], L.A. Husova[145], A. Hutson[125], J.P. Iddon[34,128], R. Ilkaev[109], H. Ilyas[14], M. Inaba[134], G.M. Innocenti[34], M. Ippolitov[89], A. Isakov[96], T. Isidori[127], M.S. Islam[110], M. Ivanov[108], V. Ivanov[99], V. Izucheev[92], M. Jablonski[2], B. Jacak[80], N. Jacazio[34], P.M. Jacobs[80], S. Jadlovska[117], J. Jadlovsky[117], S. Jaelani[62], C. Jahnke[122,121], M.J. Jakubowska[143], A. Jalotra[102], M.A. Janik[143], T. Janson[74], M. Jercic[100], O. Jevons[111], A.A.P. Jimenez[69], F. Jonas[97,145], P.G. Jones[111], J.M. Jowett[34,108], J. Jung[68], M. Jung[68], A. Junique[34], A. Jusko[111], M.J. Kabus[143], J. Kaewjai[116], P. Kalinak[64], A.S. Kalteyer[108], A. Kalweit[34], V. Kaplin[94], A. Karasu Uysal[77], D. Karatovic[100], O. Karavichev[63], T. Karavicheva[63], P. Karczmarczyk[143], E. Karpechev[63], V. Kashyap[87], A. Kazantsev[89], U. Kebschull[74], R. Keidel[47], D.L.D. Keijdener[62], M. Keil[34], B. Ketzer[43], Z. Khabanova[91], A.M. Khan[7], S. Khan[16], A. Khanzadeev[99], Y. Kharlov[92,82], A. Khatun[16], A. Khuntia[118], B. Kileng[36], B. Kim[17,61], C. Kim[17], D.J. Kim[126], E.J. Kim[73], J. Kim[148], J.S. Kim[41], J. Kim[105], J. Kim[73], M. Kim[105], S. Kim[18], T. Kim[148], S. Kirsch[68], I. Kisel[39], S. Kiselev[93], A. Kisiel[143], J.P. Kitowski[2], J.L. Klay[6], J. Klein[34], S. Klein[80], C. Klein-Bösing[145], M. Kleiner[68], T. Klemenz[106], A. Kluge[34], A.G. Knospe[125], C. Kobdaj[116], T. Kollegger[108], A. Kondratyev[75], N. Kondratyeva[94], E. Kondratyuk[92], J. Konig[68], S.A. Konigstorfer[106], P.J. Konopka[34], G. Kornakov[143], S.D. Koryciak[2], A. Kotliarov[96], O. Kovalenko[86], V. Kovalenko[113], M. Kowalski[118], I. Králik[64], A. Kravčáková[38], L. Kreis[108], M. Krivda[111,64], F. Krizek[96], K. Krizkova Gajdosova[37], M. Kroesen[105], M. Krüger[68], D.M. Krupova[37], E. Kryshen[99], M. Krzewicki[39], V. Kučera[34], C. Kuhn[138], P.G. Kuijer[91], T. Kumaoka[134], D. Kumar[142], L. Kumar[101], N. Kumar[101], S. Kundu[34], P. Kurashvili[86], A. Kurepin[63], A.B. Kurepin[63], A. Kuryakin[109], S. Kushpil[96], J. Kvapil[111], M.J. Kweon[61], J.Y. Kwon[61], Y. Kwon[148], S.L. La Pointe[39], P. La Rocca[26], Y.S. Lai[80], A. Lakrathok[116], M. Lamanna[34], R. Langoy[130], P. Larionov[34,52], E. Laudi[34], L. Lautner[34,106], R. Lavicka[114,37], T. Lazareva[113], R. Lea[141,23,58], J. Lehrbach[39], R.C. Lemmon[95], I. León Monzón[120], E.D. Lesser[19], M. Lettrich[34,106], P. Lévai[146], X. Li[11], X.L. Li[7], J. Lien[130], R. Lietava[111], B. Lim[17], S.H. Lim[17], V. Lindenstruth[39], A. Lindner[48], C. Lippmann[108], A. Liu[19], D.H. Liu[7], J. Liu[128], I.M. Lofnes[21], V. Loginov[94], C. Loizides[97], P. Loncar[35], J.A. Lopez[105], X. Lopez[136], E. López Torres[8], J.R. Luhder[145], M. Lunardon[27], G. Luparello[60], Y.G. Ma[40], A. Maevskaya[63], M. Mager[34], T. Mahmoud[43], A. Maire[138], M. Malaev[99], N.M. Malik[102], Q.W. Malik[20], S.K. Malik[102], L. Malinina[IV,75], D. Mal'Kevich[93], D. Mallick[87], N. Mallick[50], G. Mandaglio[32,56], V. Manko[89], F. Manso[136], V. Manzari[53], Y. Mao[7], G.V. Margagliotti[23], A. Margotti[54], A. Marín[108], C. Markert[119], M. Marquard[68], N.A. Martin[105], P. Martinengo[34], J.L. Martinez[125], M.I. Martínez[45], G. Martínez García[115], S. Masciocchi[108], M. Masera[24], A. Masoni[55], L. Massacrier[78], A. Mastroserio[140,53], A.M. Mathis[106], O. Matonoha[81], P.F.T. Matuoka[121], A. Matyja[118], C. Mayer[118], A.L. Mazuecos[34], F. Mazzaschi[24], M. Mazzilli[34], J.E. Mdhluli[132], A.F. Mechler[68], Y. Melikyan[63], A. Menchaca-Rocha[71], E. Meninno[114,29], A.S. Menon[125], M. Meres[13], S. Mhlanga[124,72], Y. Miake[134], L. Micheletti[59], L.C. Migliorin[137], D.L. Mihaylov[106], K. Mikhaylov[75,93], A.N. Mishra[146], D. Miśkowiec[108], A. Modak[4], A.P. Mohanty[62], B. Mohanty[87], M. Mohisin Khan[V,16], M.A. Molander[44], Z. Moravcova[90], C. Mordasini[106], D.A. Moreira De Godoy[145], I. Morozov[63], A. Morsch[34], T. Mrnjavac[34], V. Muccifora[52], E. Mudnic[35], D. Mühlheim[145], S. Muhuri[142], J.D. Mulligan[80], A. Mulliri[22], M.G. Munhoz[121], R.H. Munzer[68], H. Murakami[133], S. Murray[124], L. Musa[34], J. Musinsky[64], J.W. Myrcha[143], B. Naik[132], R. Nair[86], B.K. Nandi[49], R. Nania[54], E. Nappi[53],

A.F. Nassirpour[81], A. Nath[105], C. Nattrass[131], A. Neagu[20], A. Negru[135], L. Nellen[69], S.V. Nesbo[36], G. Neskovic[39], D. Nesterov[113], B.S. Nielsen[90], S. Nikolaev[89], S. Nikulin[89], V. Nikulin[99], F. Noferini[54], S. Noh[12], P. Nomokonov[75], J. Norman[128], N. Novitzky[134], P. Nowakowski[143], A. Nyanin[89], J. Nystrand[21], M. Ogino[83], A. Ohlson[81], V.A. Okorokov[94], J. Oleniacz[143], A.C. Oliveira Da Silva[131], M.H. Oliver[147], A. Onnerstad[126], C. Oppedisano[59], A. Ortiz Velasquez[69], T. Osako[46], A. Oskarsson[81], J. Otwinowski[118], M. Oya[46], K. Oyama[83], Y. Pachmayer[105], S. Padhan[49], D. Pagano[141,58], G. Paić[69], A. Palasciano[53], J. Pan[144], S. Panebianco[139], J. Park[61], J.E. Parkkila[126], S.P. Pathak[125], R.N. Patra[102,34], B. Paul[22], H. Pei[7], T. Peitzmann[62], X. Peng[7], L.G. Pereira[70], H. Pereira Da Costa[139], D. Peresunko[89,82], G.M. Perez[8], S. Perrin[139], Y. Pestov[5], V. Petráček[37], M. Petrovici[48], R.P. Pezzi[115,70], S. Piano[60], M. Pikna[13], P. Pillot[115], O. Pinazza[54,34], L. Pinsky[125], C. Pinto[26], S. Pisano[52], M. Płoskoń[80], M. Planinic[100], F. Pliquett[68], M.G. Poghosyan[97], B. Polichtchouk[92], S. Politano[30], N. Poljak[100], A. Pop[48], S. Porteboeuf-Houssais[136], J. Porter[80], V. Pozdniakov[75], S.K. Prasad[4], R. Preghenella[54], F. Prino[59], C.A. Pruneau[144], I. Pshenichnov[63], M. Puccio[34], S. Qiu[91], L. Quaglia[24], R.E. Quishpe[125], S. Ragoni[111], A. Rakotozafindrabe[139], L. Ramello[31], F. Rami[138], S.A.R. Ramirez[45], A.G.T. Ramos[33], T.A. Rancien[79], R. Raniwala[103], S. Raniwala[103], S.S. Räsänen[44], R. Rath[50], I. Ravasenga[91], K.F. Read[97,131], A.R. Redelbach[39], K. Redlich[VI,86], A. Rehman[21], P. Reichelt[68], F. Reidt[34], H.A. Reme-ness[36], Z. Rescakova[38], K. Reygers[105], A. Riabov[99], V. Riabov[99], T. Richert[81], M. Richter[20], W. Riegler[34], F. Riggi[26], C. Ristea[67], M. Rodríguez Cahuantzi[45], K. Røed[20], R. Rogalev[92], E. Rogochaya[75], T.S. Rogoschinski[68], D. Rohr[34], D. Röhrich[21], P.F. Rojas[45], S. Rojas Torres[37], P.S. Rokita[143], F. Ronchetti[52], A. Rosano[32,56], E.D. Rosas[69], A. Rossi[57], A. Roy[50], P. Roy[110], S. Roy[49], N. Rubini[25], O.V. Rueda[81], D. Ruggiano[143], R. Rui[23], B. Rumyantsev[75], P.G. Russek[2], R. Russo[91], A. Rustamov[88], E. Ryabinkin[89], Y. Ryabov[99], A. Rybicki[118], H. Rytkonen[126], W. Rzesa[143], O.A.M. Saarimaki[44], R. Sadek[115], S. Sadovsky[92], J. Saetre[21], K. Šafařík[37], S.K. Saha[142], S. Saha[87], B. Sahoo[49], P. Sahoo[49], R. Sahoo[50], S. Sahoo[65], D. Sahu[50], P.K. Sahu[65], J. Saini[142], S. Sakai[134], M.P. Salvan[108], S. Sambyal[102], V. Samsonov[I,99,94], T.B. Saramela[121], D. Sarkar[144], N. Sarkar[142], P. Sarma[42], V.M. Sarti[106], M.H.P. Sas[147], J. Schambach[97], H.S. Scheid[68], C. Schiaua[48], R. Schicker[105], A. Schmah[105], C. Schmidt[108], H.R. Schmidt[104], M.O. Schmidt[34,105], M. Schmidt[104], N.V. Schmidt[97,68], A.R. Schmier[131], R. Schotter[138], J. Schukraft[34], K. Schwarz[108], K. Schweda[108], G. Scioli[25], E. Scomparin[59], J.E. Seger[15], Y. Sekiguchi[133], D. Sekihata[133], I. Selyuzhenkov[108,94], S. Senyukov[138], J.J. Seo[61], D. Serebryakov[63], L. Šerkšnytė[106], A. Sevcenco[67], T.J. Shaba[72], A. Shabanov[63], A. Shabetai[115], R. Shahoyan[34], W. Shaikh[110], A. Shangaraev[92], A. Sharma[101], H. Sharma[118], M. Sharma[102], N. Sharma[101], S. Sharma[102], U. Sharma[102], A. Shatat[78], O. Sheibani[125], K. Shigaki[46], M. Shimomura[84], S. Shirinkin[93], Q. Shou[40], Y. Sibiriak[89], S. Siddhanta[55], T. Siemiarczuk[86], T.F. Silva[121], D. Silvermyr[81], T. Simantathammakul[116], G. Simonetti[34], B. Singh[106], R. Singh[87], R. Singh[102], R. Singh[50], V.K. Singh[142], V. Singhal[142], T. Sinha[110], B. Sitar[13], M. Sitta[31], T.B. Skaali[20], G. Skorodumovs[105], M. Slupecki[44], N. Smirnov[147], R.J.M. Snellings[62], C. Soncco[112], J. Song[125], A. Songmoolnak[116], F. Soramel[27], S. Sorensen[131], I. Sputowska[118], J. Stachel[105], I. Stan[67], P.J. Steffanic[131], S.F. Stiefelmaier[105], D. Stocco[115], I. Storehaug[20], M.M. Storetvedt[36], P. Stratmann[145], S. Strazzi[25], C.P. Stylianidis[91], A.A.P. Suaide[121], C. Suire[78], M. Sukhanov[63], M. Suljic[34], R. Sultanov[93], V. Sumberia[102], S. Sumowidagdo[51], S. Swain[65], A. Szabo[13], I. Szarka[13], U. Tabassam[14], S.F. Taghavi[106], G. Taillepied[136], J. Takahashi[122], G.J. Tambave[21], S. Tang[136,7], Z. Tang[129], J.D. Tapia Takaki[VII,127], M.G. Tarzila[48], A. Tauro[34], G. Tejeda Muñoz[45], A. Telesca[34], L. Terlizzi[24], C. Terrevoli[125], G. Tersimonov[3], S. Thakur[142], D. Thomas[119], R. Tieulent[137], A. Tikhonov[63], A.R. Timmins[125], M. Tkacik[117], A. Toia[68], N. Topilskaya[63], M. Toppi[52], F. Torales-Acosta[19], T. Tork[78], A. Trifiró[32,56], S. Tripathy[54,69], T. Tripathy[49], S. Trogolo[34,27], V. Trubnikov[3], W.H. Trzaska[126], T.P. Trzcinski[143], A. Tumkin[109], R. Turrisi[57], T.S. Tveter[20], K. Ullaland[21], A. Uras[137], M. Urioni[58,141], G.L. Usai[22], M. Vala[38], N. Valle[28], S. Vallero[59], L.V.R. van Doremalen[62], M. van Leeuwen[91], P. Vande Vyvre[34], D. Varga[146], Z. Varga[146], M. Varga-Kofarago[146], M. Vasileiou[85], A. Vasiliev[89], O. Vázquez Doce[52,106], V. Vechernin[113], A. Velure[21], E. Vercellin[24], S. Vergara Limón[45], L. Vermunt[62], R. Vértesi[146], M. Verweij[62], L. Vickovic[35], Z. Vilakazi[132], O. Villalobos Baillie[111], G. Vino[53],

A. Vinogradov[89], T. Virgili[29], V. Vislavicius[90], A. Vodopyanov[75], B. Volkel[34,105], M.A. Völkl[105], K. Voloshin[93], S.A. Voloshin[144], G. Volpe[33], B. von Haller[34], I. Vorobyev[106], N. Vozniuk[63], J. Vrláková[38], B. Wagner[21], C. Wang[40], D. Wang[40], M. Weber[114], R.J.G.V. Weelden[91], A. Wegrzynek[34], S.C. Wenzel[34], J.P. Wessels[145], J. Wiechula[68], J. Wikne[20], G. Wilk[86], J. Wilkinson[108], G.A. Willems[145], B. Windelband[105], M. Winn[139], W.E. Witt[131], J.R. Wright[119], W. Wu[40], Y. Wu[129], R. Xu[7], A.K. Yadav[142], S. Yalcin[77], Y. Yamaguchi[46], K. Yamakawa[46], S. Yang[21], S. Yano[46], Z. Yin[7], I.-K. Yoo[17], J.H. Yoon[61], S. Yuan[21], A. Yuncu[105], V. Zaccolo[23], C. Zampolli[34], H.J.C. Zanoli[62], N. Zardoshti[34], A. Zarochentsev[113], P. Závada[66], N. Zaviyalov[109], M. Zhalov[99], B. Zhang[7], S. Zhang[40], X. Zhang[7], Y. Zhang[129], V. Zherebchevskii[113], Y. Zhi[11], N. Zhigareva[93], D. Zhou[7], Y. Zhou[90], J. Zhu[108,7], Y. Zhu[7], G. Zinovjev[I,3], N. Zurlo[141,58]

Affiliation Notes

[I] Deceased
[II] Also at: Italian National Agency for New Technologies, Energy and Sustainable Economic Development (ENEA), Bologna, Italy
[III] Also at: Dipartimento DET del Politecnico di Torino, Turin, Italy
[IV] Also at: M.V. Lomonosov Moscow State University, D.V. Skobeltsyn Institute of Nuclear, Physics, Moscow, Russia
[V] Also at: Department of Applied Physics, Aligarh Muslim University, Aligarh, India
[VI] Also at: Institute of Theoretical Physics, University of Wroclaw, Poland
[VII] Also at: University of Kansas, Lawrence, Kansas, United States

Collaboration Institutes

[1] A.I. Alikhanyan National Science Laboratory (Yerevan Physics Institute) Foundation, Yerevan, Armenia
[2] AGH University of Science and Technology, Cracow, Poland
[3] Bogolyubov Institute for Theoretical Physics, National Academy of Sciences of Ukraine, Kiev, Ukraine
[4] Bose Institute, Department of Physics and Centre for Astroparticle Physics and Space Science (CAPSS), Kolkata, India
[5] Budker Institute for Nuclear Physics, Novosibirsk, Russia
[6] California Polytechnic State University, San Luis Obispo, California, United States
[7] Central China Normal University, Wuhan, China
[8] Centro de Aplicaciones Tecnológicas y Desarrollo Nuclear (CEADEN), Havana, Cuba
[9] Centro de Investigación y de Estudios Avanzados (CINVESTAV), Mexico City and Mérida, Mexico
[10] Chicago State University, Chicago, Illinois, United States
[11] China Institute of Atomic Energy, Beijing, China
[12] Chungbuk National University, Cheongju, Republic of Korea
[13] Comenius University Bratislava, Faculty of Mathematics, Physics and Informatics, Bratislava, Slovakia
[14] COMSATS University Islamabad, Islamabad, Pakistan
[15] Creighton University, Omaha, Nebraska, United States
[16] Department of Physics, Aligarh Muslim University, Aligarh, India
[17] Department of Physics, Pusan National University, Pusan, Republic of Korea
[18] Department of Physics, Sejong University, Seoul, Republic of Korea
[19] Department of Physics, University of California, Berkeley, California, United States

[20] Department of Physics, University of Oslo, Oslo, Norway

[21] Department of Physics and Technology, University of Bergen, Bergen, Norway

[22] Dipartimento di Fisica dell'Università and Sezione INFN, Cagliari, Italy

[23] Dipartimento di Fisica dell'Università and Sezione INFN, Trieste, Italy

[24] Dipartimento di Fisica dell'Università and Sezione INFN, Turin, Italy

[25] Dipartimento di Fisica e Astronomia dell'Università and Sezione INFN, Bologna, Italy

[26] Dipartimento di Fisica e Astronomia dell'Università and Sezione INFN, Catania, Italy

[27] Dipartimento di Fisica e Astronomia dell'Università and Sezione INFN, Padova, Italy

[28] Dipartimento di Fisica e Nucleare e Teorica, Università di Pavia, Pavia, Italy

[29] Dipartimento di Fisica 'E.R. Caianiello' dell'Università and Gruppo Collegato INFN, Salerno, Italy

[30] Dipartimento DISAT del Politecnico and Sezione INFN, Turin, Italy

[31] Dipartimento di Scienze e Innovazione Tecnologica dell'Università del Piemonte Orientale and INFN Sezione di Torino, Alessandria, Italy

[32] Dipartimento di Scienze MIFT, Università di Messina, Messina, Italy

[33] Dipartimento Interateneo di Fisica 'M. Merlin' and Sezione INFN, Bari, Italy

[34] European Organization for Nuclear Research (CERN), Geneva, Switzerland

[35] Faculty of Electrical Engineering, Mechanical Engineering and Naval Architecture, University of Split, Split, Croatia

[36] Faculty of Engineering and Science, Western Norway University of Applied Sciences, Bergen, Norway

[37] Faculty of Nuclear Sciences and Physical Engineering, Czech Technical University in Prague, Prague, Czech Republic

[38] Faculty of Science, P.J. Šafárik University, Košice, Slovakia

[39] Frankfurt Institute for Advanced Studies, Johann Wolfgang Goethe-Universität Frankfurt, Frankfurt, Germany

[40] Fudan University, Shanghai, China

[41] Gangneung-Wonju National University, Gangneung, Republic of Korea

[42] Gauhati University, Department of Physics, Guwahati, India

[43] Helmholtz-Institut für Strahlen- und Kernphysik, Rheinische Friedrich-Wilhelms-Universität Bonn, Bonn, Germany

[44] Helsinki Institute of Physics (HIP), Helsinki, Finland

[45] High Energy Physics Group, Universidad Autónoma de Puebla, Puebla, Mexico

[46] Hiroshima University, Hiroshima, Japan

[47] Hochschule Worms, Zentrum für Technologietransfer und Telekommunikation (ZTT), Worms, Germany

[48] Horia Hulubei National Institute of Physics and Nuclear Engineering, Bucharest, Romania

[49] Indian Institute of Technology Bombay (IIT), Mumbai, India

[50] Indian Institute of Technology Indore, Indore, India

[51] Indonesian Institute of Sciences, Jakarta, Indonesia

[52] INFN, Laboratori Nazionali di Frascati, Frascati, Italy

[53] INFN, Sezione di Bari, Bari, Italy

[54] INFN, Sezione di Bologna, Bologna, Italy

[55] INFN, Sezione di Cagliari, Cagliari, Italy

[56] INFN, Sezione di Catania, Catania, Italy

[57] INFN, Sezione di Padova, Padova, Italy

[58] INFN, Sezione di Pavia, Pavia, Italy

[59] INFN, Sezione di Torino, Turin, Italy

[60] INFN, Sezione di Trieste, Trieste, Italy

[61] Inha University, Incheon, Republic of Korea

[62] Institute for Gravitational and Subatomic Physics (GRASP), Utrecht University/Nikhef, Utrecht,

Netherlands

[63] Institute for Nuclear Research, Academy of Sciences, Moscow, Russia

[64] Institute of Experimental Physics, Slovak Academy of Sciences, Košice, Slovakia

[65] Institute of Physics, Homi Bhabha National Institute, Bhubaneswar, India

[66] Institute of Physics of the Czech Academy of Sciences, Prague, Czech Republic

[67] Institute of Space Science (ISS), Bucharest, Romania

[68] Institut für Kernphysik, Johann Wolfgang Goethe-Universität Frankfurt, Frankfurt, Germany

[69] Instituto de Ciencias Nucleares, Universidad Nacional Autónoma de México, Mexico City, Mexico

[70] Instituto de Física, Universidade Federal do Rio Grande do Sul (UFRGS), Porto Alegre, Brazil

[71] Instituto de Física, Universidad Nacional Autónoma de México, Mexico City, Mexico

[72] iThemba LABS, National Research Foundation, Somerset West, South Africa

[73] Jeonbuk National University, Jeonju, Republic of Korea

[74] Johann-Wolfgang-Goethe Universität Frankfurt Institut für Informatik, Fachbereich Informatik und Mathematik, Frankfurt, Germany

[75] Joint Institute for Nuclear Research (JINR), Dubna, Russia

[76] Korea Institute of Science and Technology Information, Daejeon, Republic of Korea

[77] KTO Karatay University, Konya, Turkey

[78] Laboratoire de Physique des 2 Infinis, Irène Joliot-Curie, Orsay, France

[79] Laboratoire de Physique Subatomique et de Cosmologie, Université Grenoble-Alpes, CNRS-IN2P3, Grenoble, France

[80] Lawrence Berkeley National Laboratory, Berkeley, California, United States

[81] Lund University Department of Physics, Division of Particle Physics, Lund, Sweden

[82] Moscow Institute for Physics and Technology, Moscow, Russia

[83] Nagasaki Institute of Applied Science, Nagasaki, Japan

[84] Nara Women's University (NWU), Nara, Japan

[85] National and Kapodistrian University of Athens, School of Science, Department of Physics , Athens, Greece

[86] National Centre for Nuclear Research, Warsaw, Poland

[87] National Institute of Science Education and Research, Homi Bhabha National Institute, Jatni, India

[88] National Nuclear Research Center, Baku, Azerbaijan

[89] National Research Centre Kurchatov Institute, Moscow, Russia

[90] Niels Bohr Institute, University of Copenhagen, Copenhagen, Denmark

[91] Nikhef, National institute for subatomic physics, Amsterdam, Netherlands

[92] NRC Kurchatov Institute IHEP, Protvino, Russia

[93] NRC «Kurchatov»Institute - ITEP, Moscow, Russia

[94] NRNU Moscow Engineering Physics Institute, Moscow, Russia

[95] Nuclear Physics Group, STFC Daresbury Laboratory, Daresbury, United Kingdom

[96] Nuclear Physics Institute of the Czech Academy of Sciences, Řež u Prahy, Czech Republic

[97] Oak Ridge National Laboratory, Oak Ridge, Tennessee, United States

[98] Ohio State University, Columbus, Ohio, United States

[99] Petersburg Nuclear Physics Institute, Gatchina, Russia

[100] Physics department, Faculty of science, University of Zagreb, Zagreb, Croatia

[101] Physics Department, Panjab University, Chandigarh, India

[102] Physics Department, University of Jammu, Jammu, India

[103] Physics Department, University of Rajasthan, Jaipur, India

[104] Physikalisches Institut, Eberhard-Karls-Universität Tübingen, Tübingen, Germany

[105] Physikalisches Institut, Ruprecht-Karls-Universität Heidelberg, Heidelberg, Germany

[106] Physik Department, Technische Universität München, Munich, Germany

[107] Politecnico di Bari and Sezione INFN, Bari, Italy

[108] Research Division and ExtreMe Matter Institute EMMI, GSI Helmholtzzentrum für

Schwerionenforschung GmbH, Darmstadt, Germany

[109] Russian Federal Nuclear Center (VNIIEF), Sarov, Russia

[110] Saha Institute of Nuclear Physics, Homi Bhabha National Institute, Kolkata, India

[111] School of Physics and Astronomy, University of Birmingham, Birmingham, United Kingdom

[112] Sección Física, Departamento de Ciencias, Pontificia Universidad Católica del Perú, Lima, Peru

[113] St. Petersburg State University, St. Petersburg, Russia

[114] Stefan Meyer Institut für Subatomare Physik (SMI), Vienna, Austria

[115] SUBATECH, IMT Atlantique, Université de Nantes, CNRS-IN2P3, Nantes, France

[116] Suranaree University of Technology, Nakhon Ratchasima, Thailand

[117] Technical University of Košice, Košice, Slovakia

[118] The Henryk Niewodniczanski Institute of Nuclear Physics, Polish Academy of Sciences, Cracow, Poland

[119] The University of Texas at Austin, Austin, Texas, United States

[120] Universidad Autónoma de Sinaloa, Culiacán, Mexico

[121] Universidade de São Paulo (USP), São Paulo, Brazil

[122] Universidade Estadual de Campinas (UNICAMP), Campinas, Brazil

[123] Universidade Federal do ABC, Santo Andre, Brazil

[124] University of Cape Town, Cape Town, South Africa

[125] University of Houston, Houston, Texas, United States

[126] University of Jyväskylä, Jyväskylä, Finland

[127] University of Kansas, Lawrence, Kansas, United States

[128] University of Liverpool, Liverpool, United Kingdom

[129] University of Science and Technology of China, Hefei, China

[130] University of South-Eastern Norway, Tonsberg, Norway

[131] University of Tennessee, Knoxville, Tennessee, United States

[132] University of the Witwatersrand, Johannesburg, South Africa

[133] University of Tokyo, Tokyo, Japan

[134] University of Tsukuba, Tsukuba, Japan

[135] University Politehnica of Bucharest, Bucharest, Romania

[136] Université Clermont Auvergne, CNRS/IN2P3, LPC, Clermont-Ferrand, France

[137] Université de Lyon, CNRS/IN2P3, Institut de Physique des 2 Infinis de Lyon, Lyon, France

[138] Université de Strasbourg, CNRS, IPHC UMR 7178, F-67000 Strasbourg, France, Strasbourg, France

[139] Université Paris-Saclay Centre d'Etudes de Saclay (CEA), IRFU, Départment de Physique Nucléaire (DPhN), Saclay, France

[140] Università degli Studi di Foggia, Foggia, Italy

[141] Università di Brescia, Brescia, Italy

[142] Variable Energy Cyclotron Centre, Homi Bhabha National Institute, Kolkata, India

[143] Warsaw University of Technology, Warsaw, Poland

[144] Wayne State University, Detroit, Michigan, United States

[145] Westfälische Wilhelms-Universität Münster, Institut für Kernphysik, Münster, Germany

[146] Wigner Research Centre for Physics, Budapest, Hungary

[147] Yale University, New Haven, Connecticut, United States

[148] Yonsei University, Seoul, Republic of Korea